

Current Scientific Issues in Large Scale Atmospheric Dynamics

(NASA-CP-2410) CURRENT SCIENTIFIC ISSUES IN
LARGE SCALE ATMOSPHERIC DYNAMICS (NASA)
46 p HC A03/MF A01

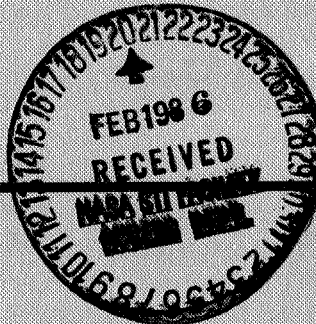
N86-24082
THRU
N86-24088
Unclas
04002

G3/47

1N
1+6



*Proceedings of a workshop held at the
NASA George C. Marshall Space Flight Center
Marshall Space Flight Center, Alabama
June 20-21, 1985*



NASA

NASA Conference Publication 2410

Current Scientific Issues in Large Scale Atmospheric Dynamics

Timothy L. Miller, *Compiler*
George C. Marshall Space Flight Center
Marshall Space Flight Center, Alabama

Proceedings of a workshop held at the
NASA George C. Marshall Space Flight Center
Marshall Space Flight Center, Alabama
June 20–21, 1985

NASA
National Aeronautics
and Space Administration

**Scientific and Technical
Information Branch**

1986

✓ 10/10

TABLE OF CONTENTS

	Page
I. INTRODUCTION AND ACKNOWLEDGMENTS (Timothy L. Miller).....	1
II. WORKSHOP PARTICIPANTS	3
III. ABSTRACTS OF PAPERS PRESENTED.....	5
Observed Aspects of Atmospheric Blocking (Stephen J. Colucci)	5
Influence of Transient Baroclinic Eddies on Planetary-Scale Waves (Lee E. Branscome)	17
Cyclogenesis (Rainer Bleck)	23
Effects of Orography on Planetary Scale Flow (Ronald B. Smith)	25
Small Scale Frontal Structure: Dynamics or Details? (David B. Parsons)	29
Simulations of Gravity Waves in Frontal Zones (Robert Gall)	37

PRECEDING PAGE BLANK NOT FILMED

I. INTRODUCTION AND ACKNOWLEDGMENTS

Timothy Lee Miller
Organizer and Chairman
Atmospheric Sciences Division
George C. Marshall Space Flight Center
Marshall Space Flight Center, Alabama 35812

This workshop was held for the purpose of exploring areas of research in global scale atmospheric dynamics which might be valuable additions to the research program of the Atmospheric Sciences Division at Marshall Space Flight Center and to the OSSA Global Scale Atmospheric Processes Research Program. The approach was to assemble a small group of research scientists to examine some specific topics, and to have a mix of observational and theoretical researchers. The meeting was kept as informal as possible to allow the participants to feel free to have discussion during, as well as after, the talks. The observationalists were chosen to be among those who were felt to be able to work well with theoreticians (or who, in fact, had themselves done some amount of theoretical work). The reasoning behind the approach of gathering these two groups together was that, if NASA wants to expand its efforts in dynamical meteorology, the theoretical work should be closely tied with space technology, and hence, with observations. Furthermore, theoretical work in general is more valuable if it is done in cooperation with observational studies. We at MSFC are interested in supporting theoretical work because it can provide support for "satellite meteorology" by providing dynamical explanations for phenomena observed with space-based sensors, and also by providing valuable input to the definitions of requirements for future space-based sensors. Finally, this approach for the workshop was attractive from an "academic" viewpoint, since it is rare that these two groups get together in this sort of structured, but informal, setting.

The topics chosen were (1) persistent anomalies ("blocking"), (2) cyclogenesis and mountain effects, and (3) frontal dynamics. It was noted during the conference that these three topics, listed in the order given above, have decreasing spatial scales, but all have important implications for global-scale atmospheric processes. The blocking phenomenon is itself a "global-scale" process, although smaller scale disturbances may be fundamental to the process. Regarding the second topic, the effects of even mesoscale mountains are important to the large scale features, as explained by Ron Smith. In the case of frontal dynamics, the front itself is usually the result of a synoptic scale phenomenon.

The workshop was successful from the viewpoint of both the NASA and the invited participants. The mix of people and meeting format seemed to give the anticipated result: plenty of stimulating discussion and debate. The comments from the participants about the workshop were quite positive. Besides discussion of the technical points as we went along, there was a general discussion near the end of the workshop about the need for theoretical workers to become more involved with data analysis and for easier access to the data by the researchers.

Most of the speaker talks and participant discussion were recorded on audio cassette tapes, and these will be made available upon request to those who might want to use them.

Acknowledgments

The idea to have a workshop was Dr. George Fichtl's (Chief, Fluid Dynamics Branch). The support and encouragement of Dr. William Vaughan, Atmospheric Sciences Division Chief, is gratefully acknowledged. The development of the approach and choice of topics were done in consultation with the participants. (Prof. Albert Barcilon deserves special mention for his working with us on this.) The responsibility for the final choice of topics and of participants is my own. Besides the talks whose abstracts are included here, George Fichtl gave an overview of the Global Scale Research Program, Pete Robertson and Dan Fitzjarrald talked about the MSFC activities in remote sensing, and Dr. John Hart showed some slides and a motion picture of flows seen on the Spacelab 3 convection experiment, the Geophysical Fluid Flow Cell.

II. WORKSHOP PARTICIPANTS

From outside of Marshall Space Flight Center:

Dr. Albert Barcilon
Geophysical Fluid Dynamics Institute
Florida State University

Dr. Rainer Bleck
Rosentiel School of Marine and Atmospheric Science
University of Miami

Dr. Lee Branscome
Rosentiel School of Marine and Atmospheric Science
University of Miami

Dr. George Chimonas
School of Geophysical Sciences
Georgia Institute of Technology

Dr. Stephen Colucci
Department of Environmental Sciences
University of Virginia

Dr. Robert Gall
Institute of Atmospheric Physics
University of Arizona

Dr. John Hart
Department of Astrophysical, Planetary, and Atmospheric Sciences
University of Colorado

Dr. Arthur Loesch
Department of Atmospheric Science
State University of New York at Albany

Dr. Terry Nathan
Department of Atmospheric Science
State University of New York at Albany

Dr. David B. Parsons
National Center for Atmospheric Research

Dr. Richard Pfeffer
Geophysical Fluid Dynamics Institute
Florida State University

Dr. Ronald Smith
Department of Geology and Geophysics
Yale University

From Atmospheric Sciences Division, Marshall Space Flight Center:

Fluid Dynamics Branch:

Dr. George Fichtl
Ms. Barbara Chance
Mr. John Kaufman
Dr. Fred Leslie
Dr. Timothy Miller
Mr. Nathaniel Reynolds (USRA)

Atmospheric Physics Branch:

Dr. Daniel Fitzjarrald
Dr. F. R. (Pete) Robertson
Dr. Jeffrey Rothermel (USRA)

III. ABSTRACTS OF PAPERS PRESENTED

OBSERVED ASPECTS OF ATMOSPHERIC BLOCKING

Stephen J. Colucci
 Department of Environmental Sciences
 University of Virginia
 Charlottesville, Virginia 22903

Atmospheric blocking has been traditionally defined as the persistence of large-scale meridional flow in the middle troposphere, such that smaller (synoptic) scale disturbances imbedded in the flow and associated with migratory surface weather systems are deflected or blocked from their normal zonal motion. Such flow regimes typically manifest themselves as quasi-stationary high amplitude planetary waves in the mid-tropospheric geopotential height fields. Should these stationary waves be sufficiently tenacious, then they may become persistent anomalies, as defined by Dole (Ph.D. thesis, MIT, 1982)¹ to consist of at least 100 meter departures from normal geopotential heights persisting for at least ten days. The structure and climatology of blocks and persistent anomalies have been well documented; there is a preference for these systems to be observed at middle and high latitudes over the oceanic regions of the northern hemisphere during the cool season. Figure 1(a) shows Dole's composite of Pacific positive anomalies in the 500 mb geopotential height field; this structure is a ridge over the central Pacific Ocean, although it sometimes can evolve into a closed anticyclonic vortex. Figure 1(b) depicts the composited Pacific negative anomalies, manifested by a closed cyclonic vortex over the central Pacific Ocean. Similar structures are observed over the Atlantic Ocean as well.

An important problem in large-scale atmospheric dynamics is understanding the evolution of these blocking systems. Inspection of a large number of cases of 500 mb cyclonic and anticyclonic blocking vortices during recent winter seasons reveals that the occurrence of these systems is preceded by high amplitude (but not necessarily stationary) planetary waves at 500 mb and by intense synoptic-scale surface cyclone activity. A possible relationship between the cyclones and planetary waves during block evolution is thus hypothesized. Detailed diagnostic study of blocking cases during January 1977, February 1978 and November 1980 discloses that the development of 500 mb anticyclonic blocking vortices is preceded in time by the intense surface cyclogenesis between 500 mb planetary scale troughs and ridges, whereas blocking cyclonic vortices form following cyclogenesis near the axes of 500 mb troughs. A positive feedback between the cyclone and planetary waves is thus implied.

The 500 mb height changes accompanying the above processes have been analyzed in terms of quasi-geostrophic potential vorticity. During anticyclonic vortex development, there are spatially and temporally persistent calculated quasi-geostrophic height rises due to anticyclonic potential vorticity advections occurring near the cyclone track. Similarly, during cyclonic vortex development, there are spatially and temporally persistent calculated quasi-geostrophic height falls due to cyclonic potential vorticity advections occurring near the cyclone track. During the breakdown of the November 1980 block, in which the cyclonic vortex is ejected downstream, the calculated quasi-geostrophic height rises near the surface cyclones are neither spatially nor temporally persistent, favoring neither blocking ridge nor trough development.

1. Also, see Large-Scale Dynamical Processes in the Atmosphere, B. Hoskins and R. Peance, editors.

Blocking and cyclone events during January 1979 have been recently diagnosed in the same manner as described above. The development of an anticyclonic vortex at 500 mb over the Atlantic Ocean is illustrated schematically by Figure 2, which shows the 5460 m height contour at two time periods one week apart. Large height rises are apparent east of Greenland where the 500 mb anticyclonic vortex is observed, while smaller (in magnitude) height falls are noted near eastern North America. On this contour analysis is superimposed the track of a major surface cyclone occurring during this week.

Large (in excess of 60 meters per twelve hours in magnitude) quasi-geostrophic height tendencies, χ_Q , during this event over the region of interest are shown in Figure 3. Large calculated height falls coincide with the storm track, as one would expect theoretically. Their centers migrate rapidly eastward until the end of the event, only at which time they may be regarded as spatially and temporally persistent; hence only moderate trough amplification is noted in Figure 2. On the other hand, large positive χ_Q centers east of the storm track persist in one region during this event, possibly accounting for the large observed ridge amplification.

During the next five days (Fig. 4), the Atlantic ridge drifts westward and the Canadian trough evolves into cyclonic vortex over the Atlantic Ocean. This coincides with a second major cyclone event. Large negative χ_Q centers are superimposed on the cyclone during its rapid intensification stage (Fig. 5), but then become detached from the cyclone and drift eastward toward the region in which the cyclonic vortex develops. Large positive χ_Q centers are observed east of the storm track and in the region toward which the blocking ridge retrogresses.

Thereafter (Fig. 6), the anticyclonic vortex weakens and a large blocking trough develops over eastern North America. Only large negative χ_Q centers (Fig. 7) are noted during this period, coinciding with a strong cyclone which is observed near the trough axis in this event rather than between the trough and ridge axes as in the previous events. The North American cyclonic vortex is dislodged, curiously, during the much-studied President's Day cyclone in mid-February. This particular process warrants further investigation.

Based on these observations, the view is advanced that blocking and cyclogenesis in some cases are part of the same process. Specifically, baroclinically active synoptic-scale waves, imbedded in amplified planetary waves, may evolve into blocking structures (cyclonic and anticyclonic vortices) having a scale intermediate between that of the original synoptic and planetary scale waves. This is consistent with Dole's observation of persistent anomaly evolution; these systems originate as transient baroclinic systems which evolve into stationary, amplified equivalent barotropic structures. Figure 8, from Dole's Ph.D. thesis, shows the time evolution of the Pacific negative anomaly, for example. The corresponding surface pressure and tropospheric thickness pattern evolution in Figure 9 clearly illustrates the baroclinicity of these systems.

Further observational research should be devoted to exploring possible synoptic-to-planetary scale couplings in other blocking events and understanding large-scale circulation changes which accompany surface cyclogenesis. The role of tropical-to-mid-latitude interactions during these events needs to be investigated; there is tentative evidence during the January 1979 episode that streams of anticyclonic

potential vorticity emanating from the tropics were being trapped by the mid-latitude cyclones. Whether these streams were coupled with tropical cloudiness or moisture invites additional inquiry. Theoretical effort should be aimed at understanding the nature of local interactions between synoptic and planetary scale waves such as that which appears to be observed during the blocking process as proposed here.

**ORIGINAL PAGE IS
OF POOR QUALITY**

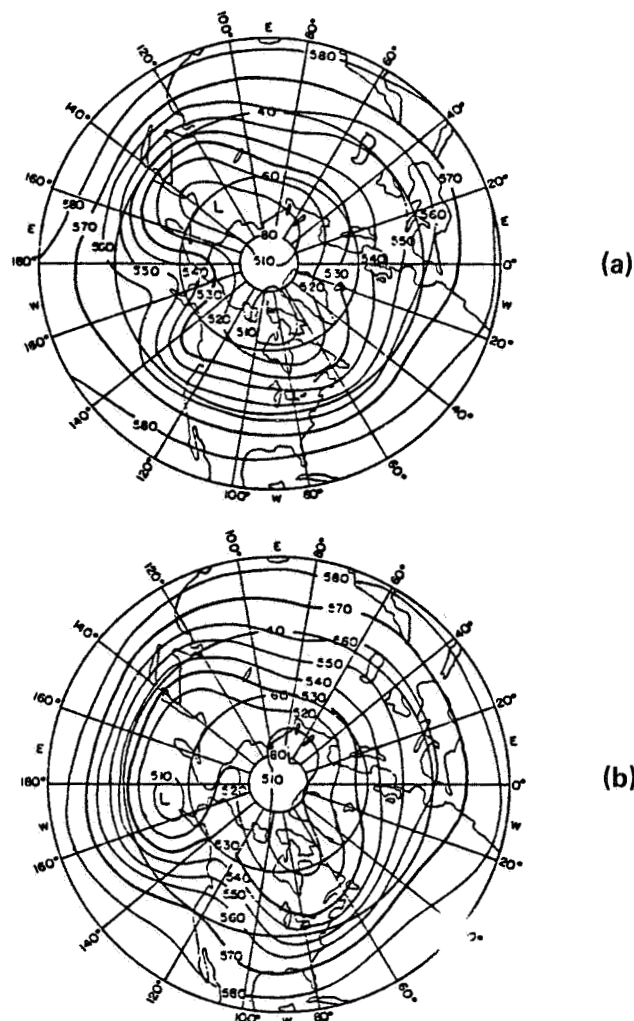
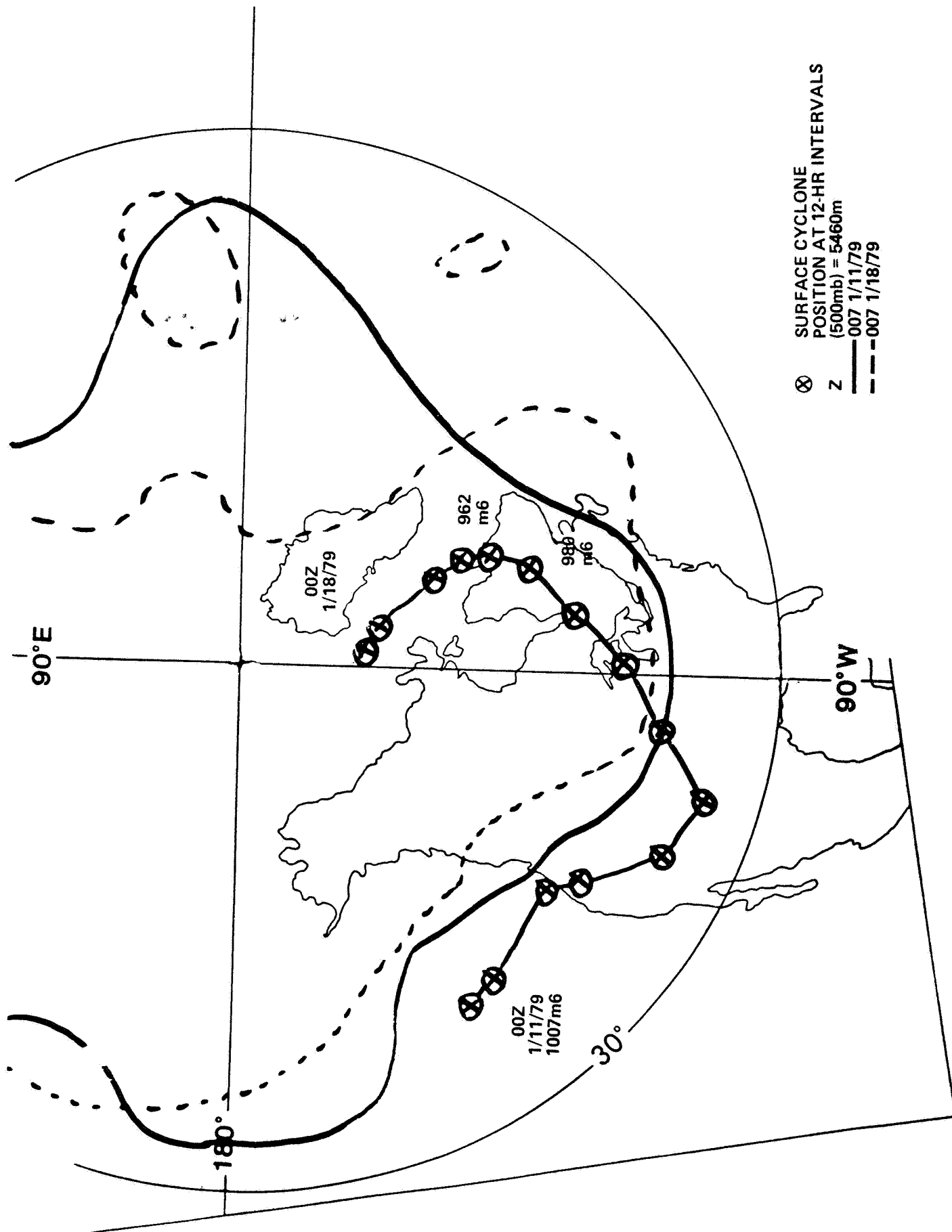


Figure 1. Persistent positive (a) and negative (b) anomaly composites for the Pacific Ocean (from Dole's Ph.D. Thesis).



⊗ SURFACE CYCLONE
 POSITION AT 12-HR INTERVALS
 Z (500mb) = 5460m
 — 007 1/11/79
 --- 007 1/18/79

Figure 2.

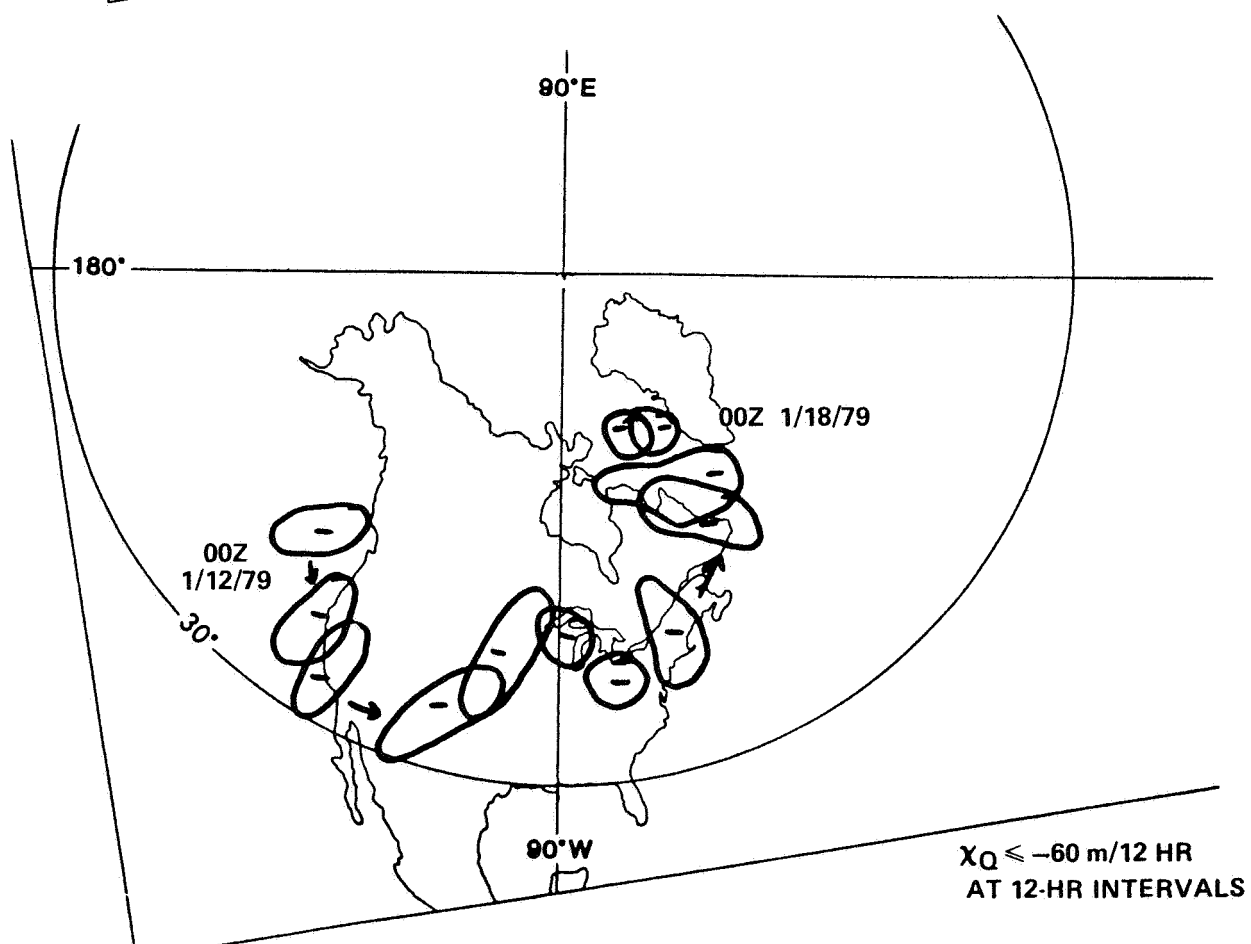
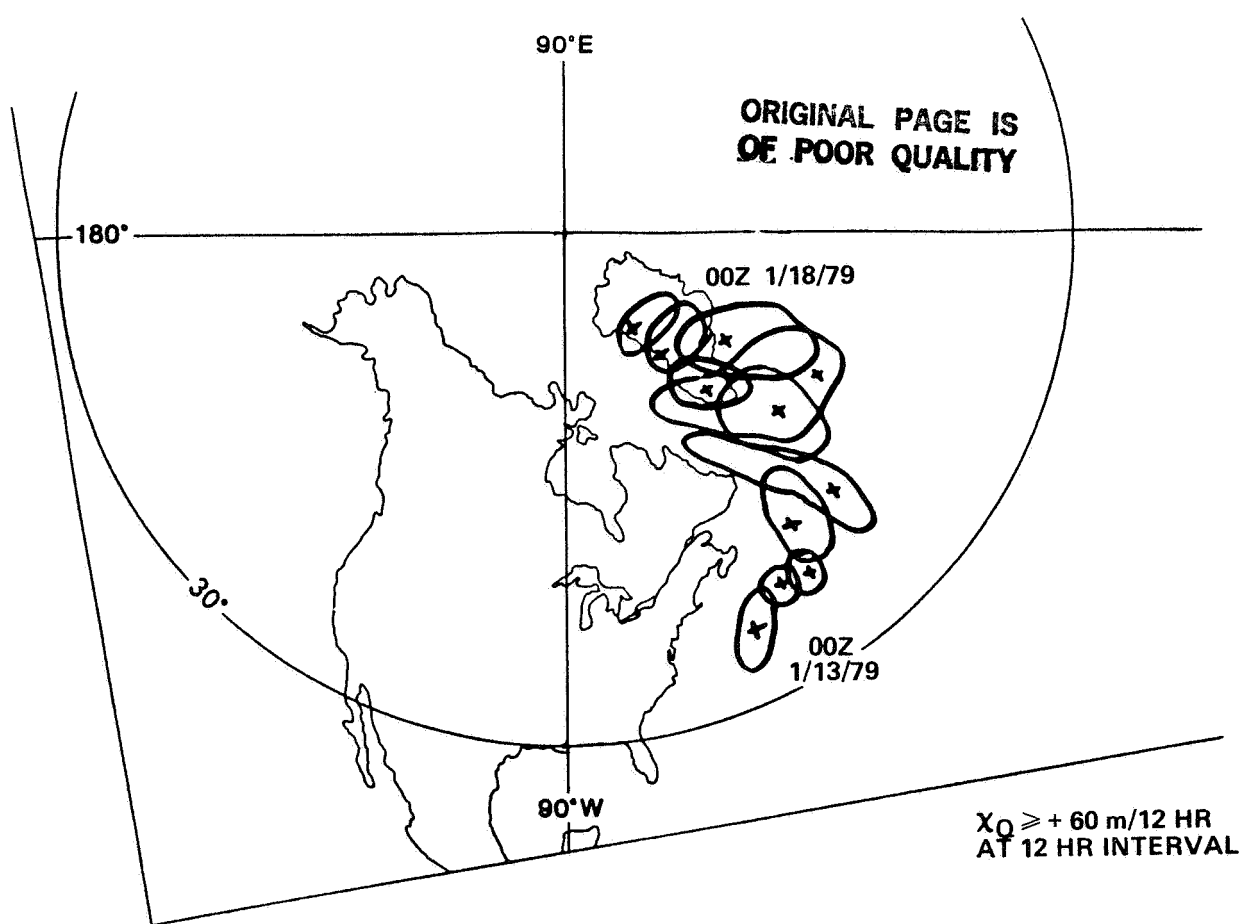


Figure 3

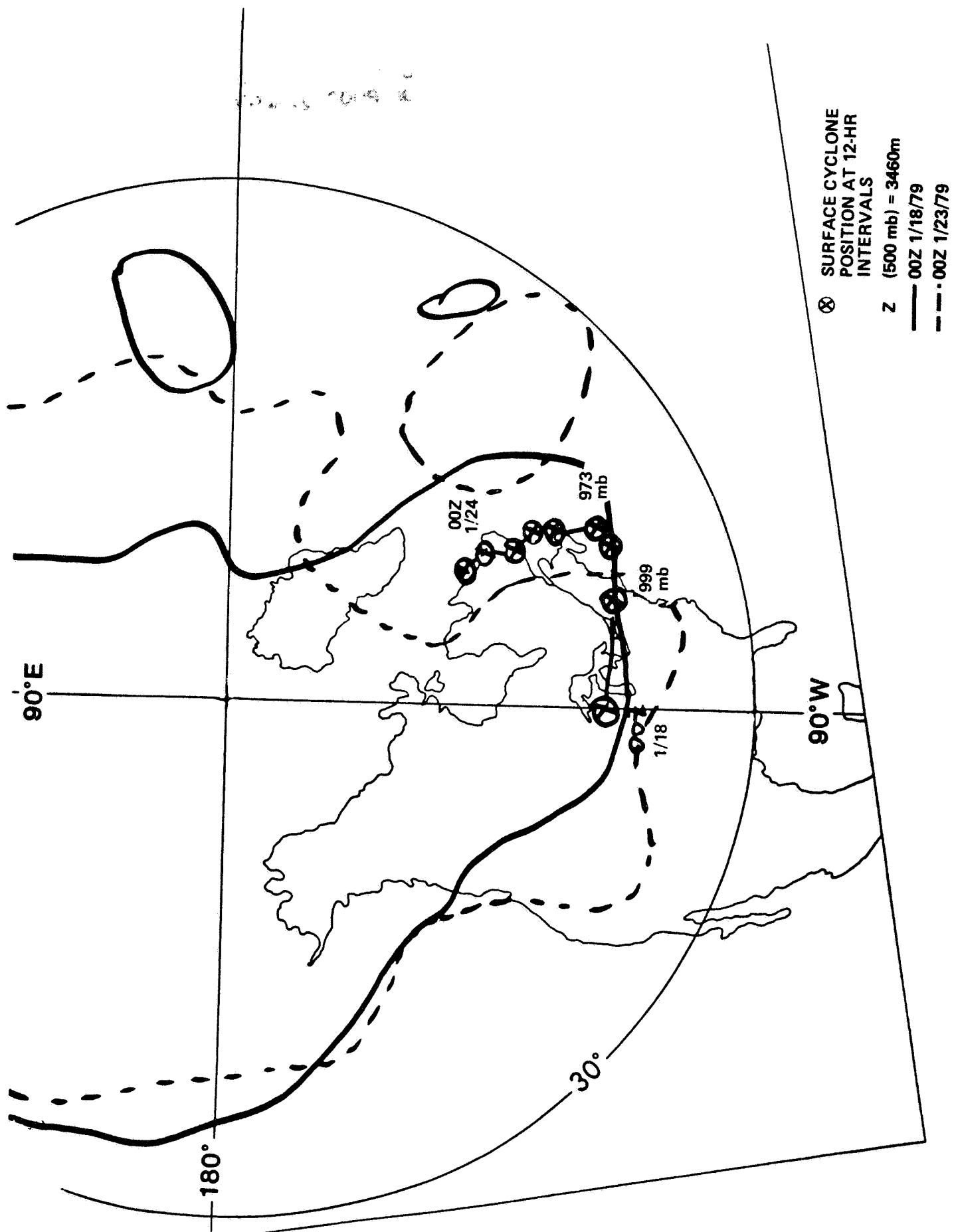


Figure 4

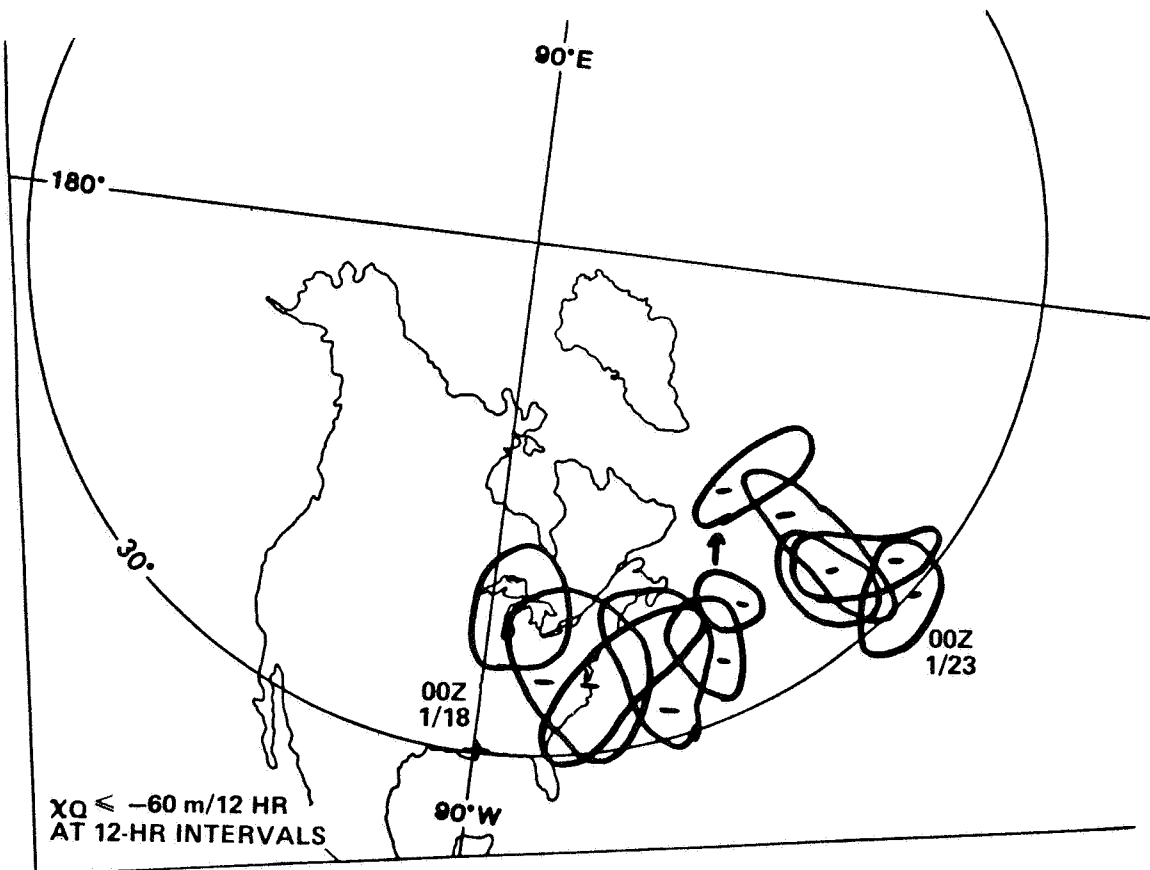
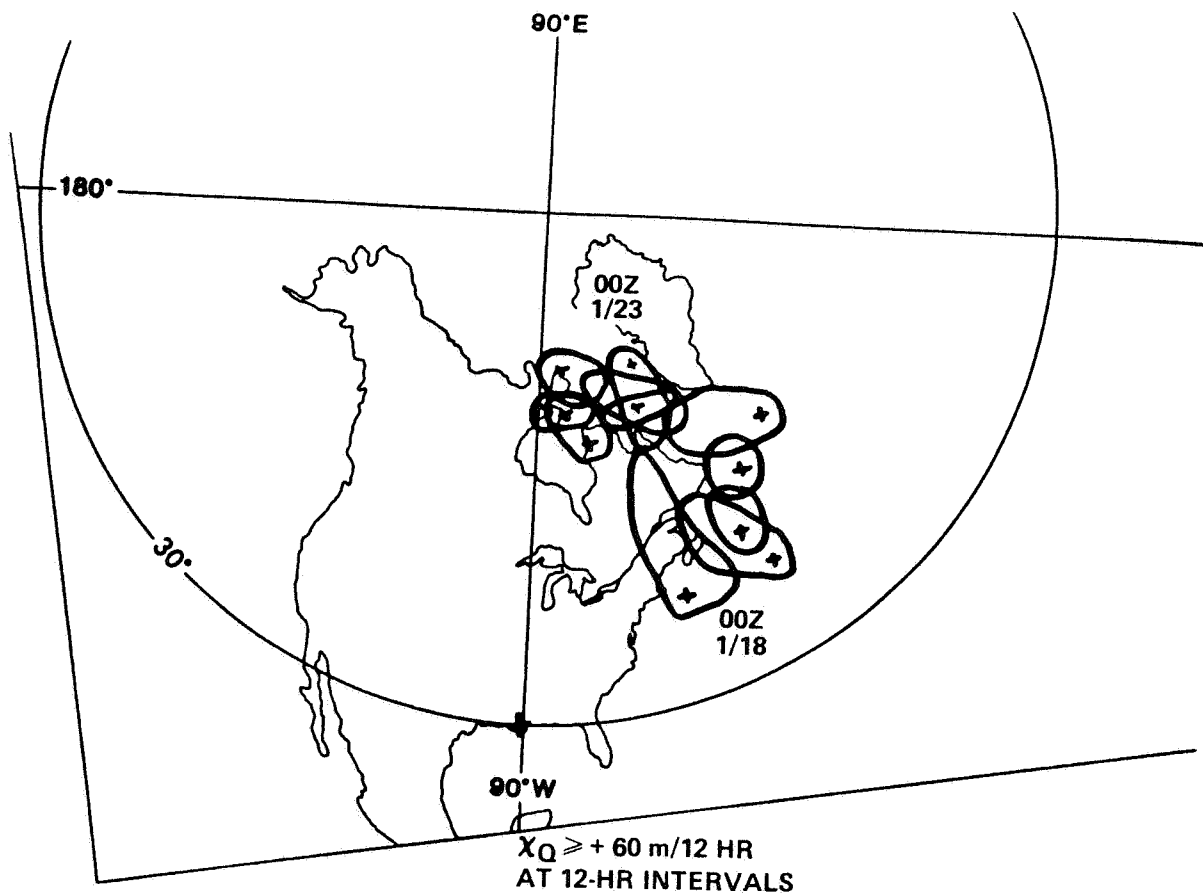


Figure 5

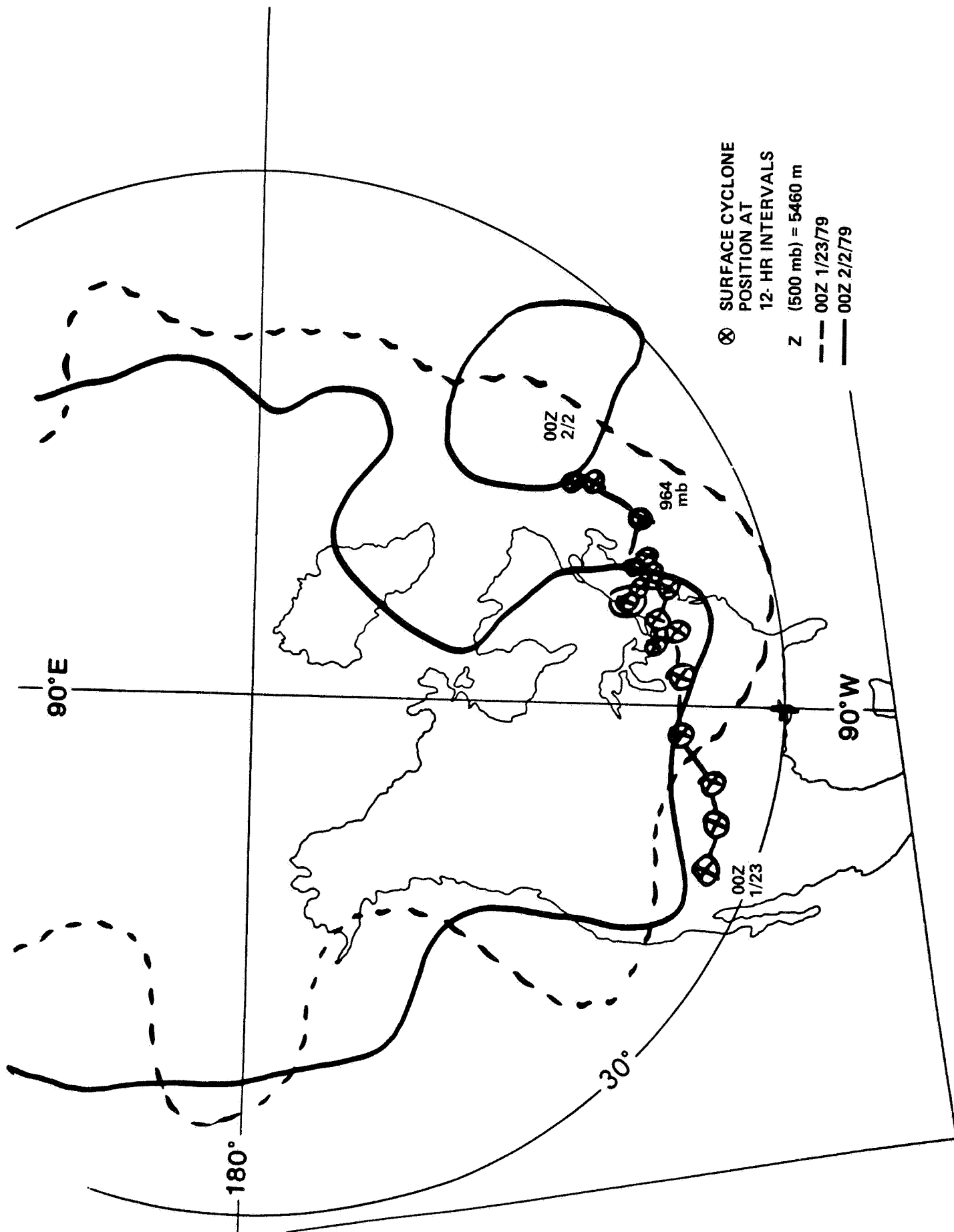


Figure 6

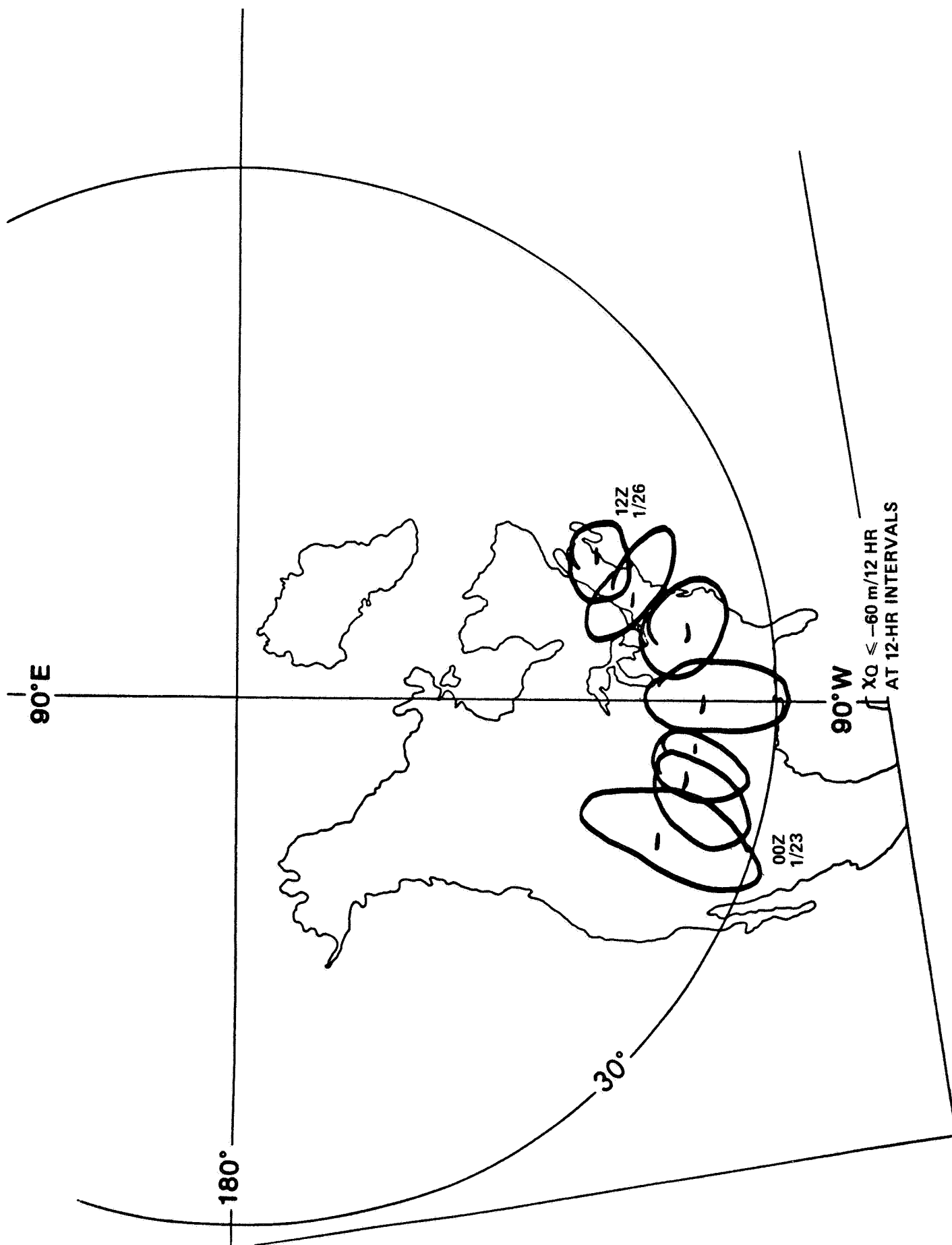


Figure 7

PAC – CASES – 500 mb Z

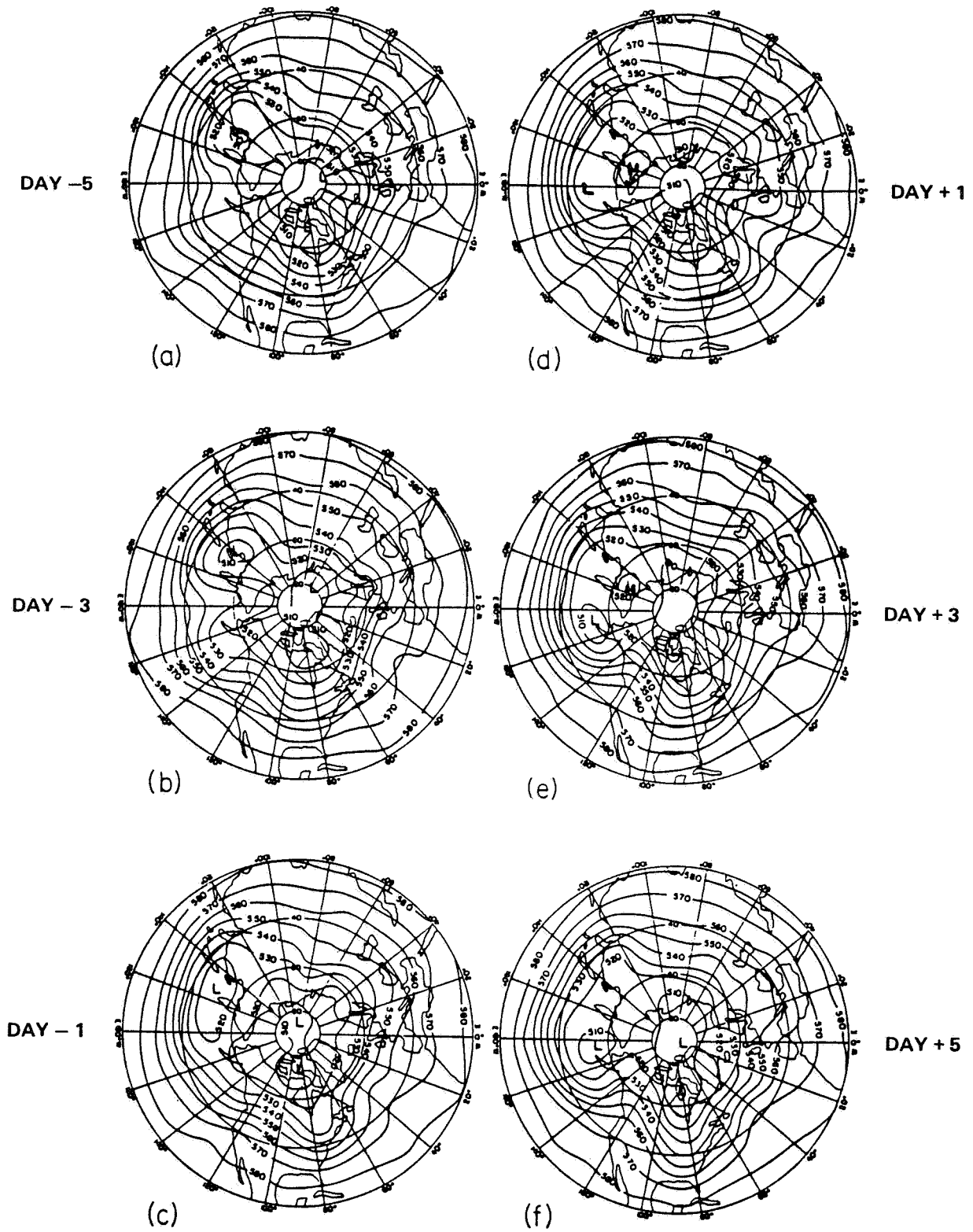
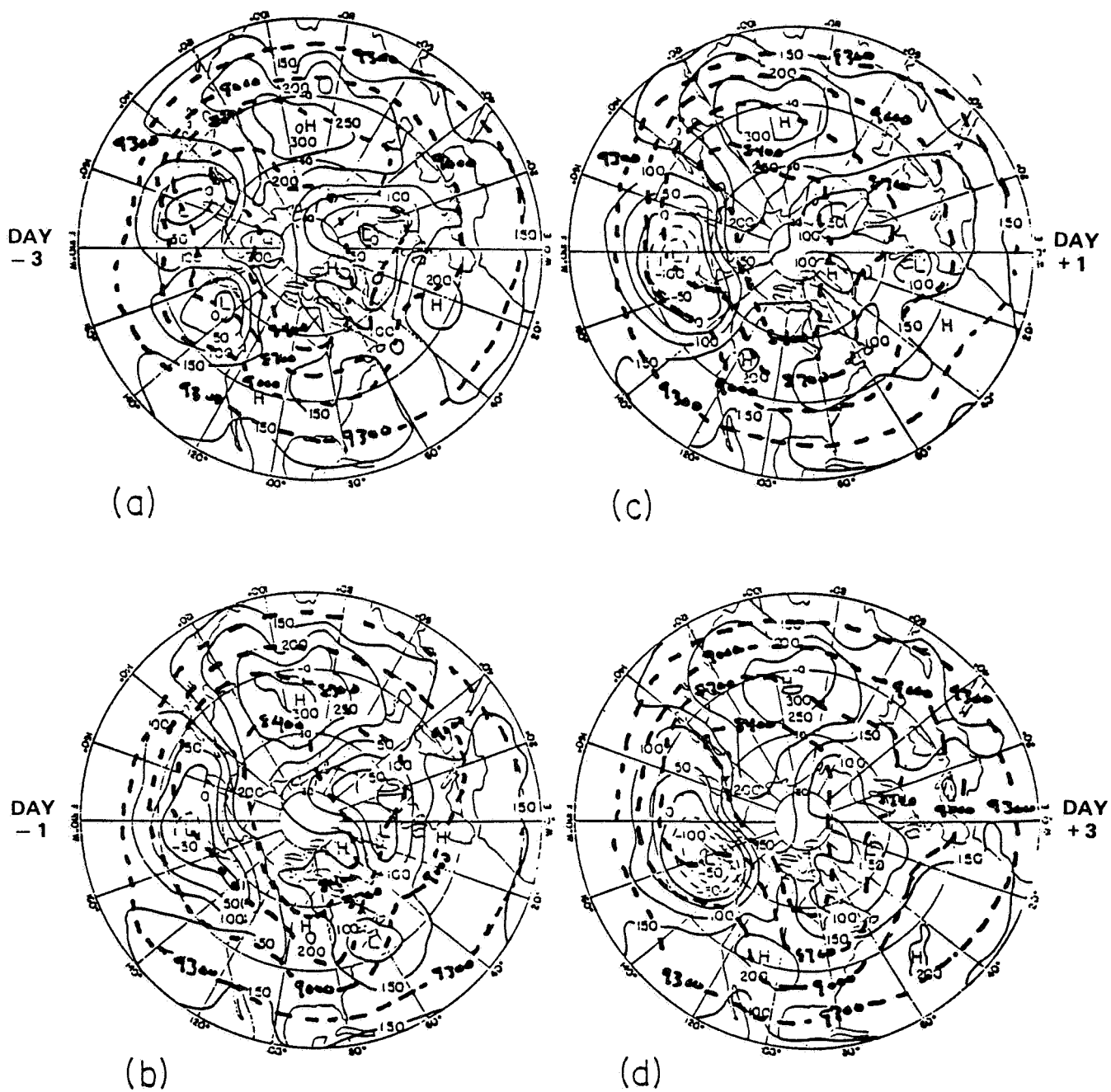


Figure 8

PAC -
1000 mb Z ———
1000 mb - 300 mb OZ - - -



2

3

4

5

6

7

INFLUENCE OF TRANSIENT BAROCLINIC EDDIES
ON PLANETARY-SCALE WAVESLee E. Branscome
University of Miami
RSMAS-MPO

Low-order models with a mean zonal flow forced by zonally symmetric heating and one planetary-scale wave forced by topography have multiple flow equilibria (Charney and Devore, 1979; Charney and Straus, 1980). Two stable equilibria are characterized by strong zonal flow with low wave amplitude (high index circulation) and weak zonal flow with a high wave amplitude (low index circulation) fixed in phase with the topography. These two states presumably represent "normal" zonal circulation and a "blocking" configuration, respectively.

When a shorter, baroclinically unstable wave is added to this low-order model, the planetary-scale wave no longer stays in stable equilibrium states (Reinhold and Pierrehumbert, 1982). Instead, the long wave remains in "weather regimes" or preferred regions in phase space (Fig. 1). These regimes are, in general, different from the equilibria of the model with the planetary-scale wave only. Thus, the short unstable wave adds some randomness to planetary-scale circulation and changes its position with respect to the planetary-scale topography.

The Reinhold and Pierrehumbert model is further explored here by adding a long-wave in the thermal forcing and exploring wider parameter space. When the symmetric thermal forcing is weak so that the short wave is stable, the planetary-scale wave is fixed in amplitude and phase by the asymmetric forcing (Fig. 2). However, when the symmetric forcing is increased to an unstable level, the planetary-scale wave becomes less organized. With asymmetric thermal forcing only (i.e., no topography) the long-wave is randomly distributed through phase space (Fig. 3). Thermal forcing seems to be less effective in organizing "weather regimes" than topographic forcing.

In some cases, a limit cycle occurs in the planetary-scale wave activity (Fig. 4). The wave behavior is distinctly different from Figure 3 which lacks topography and is randomly distributed and from Figure 1 which lacks asymmetric thermal forcing and has no limit cycle. Topography is necessary to create "weather regimes," but they will be qualitatively altered by asymmetric thermal forcing. The cross in Figure 4 shows the position of the forced wave with stable zonal flow (i.e., when the short wave is stable). Again, the unstable short wave can drastically alter the long-wave behavior.

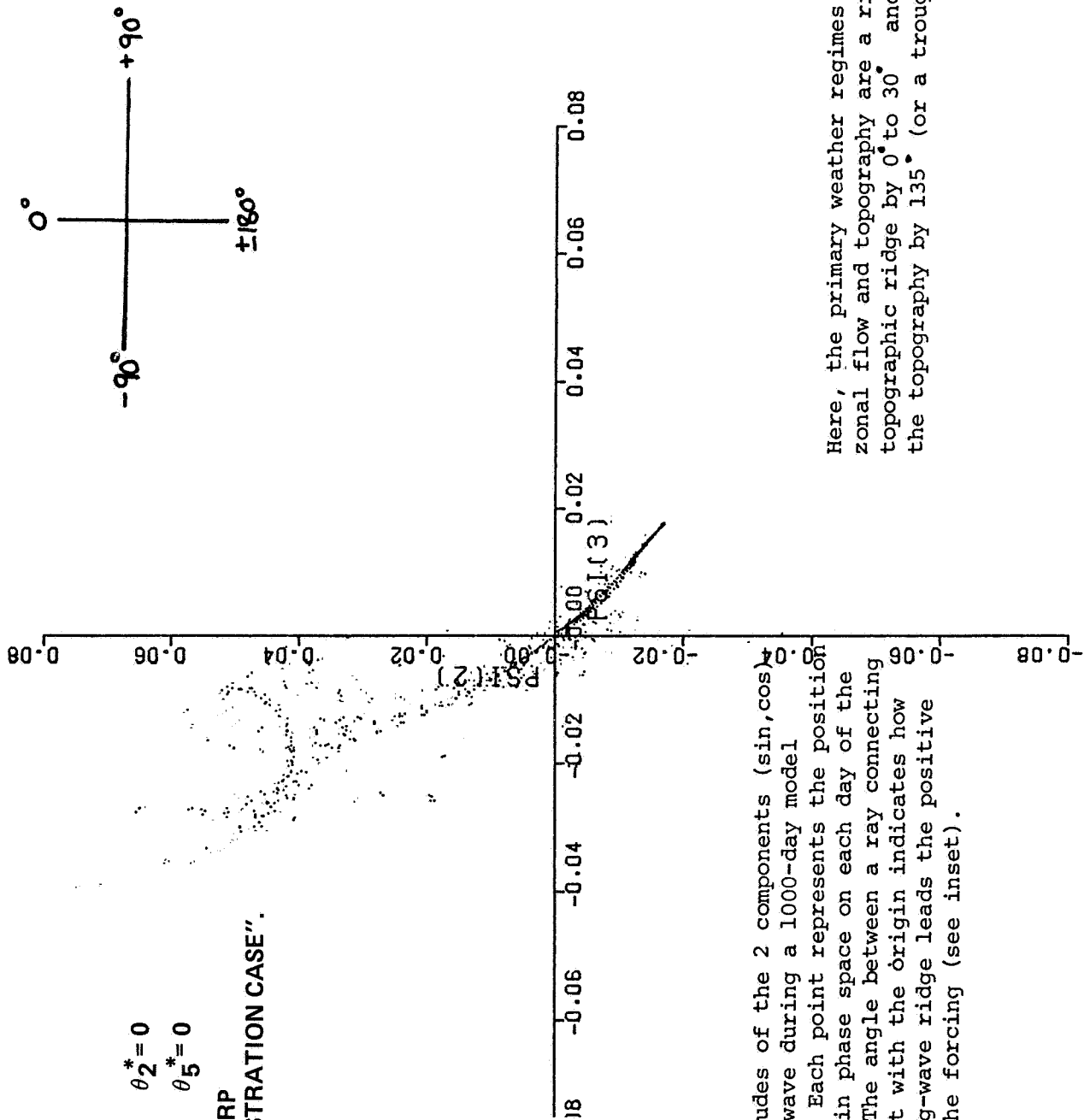
This low-order model shows the importance of interaction of topography and thermal forcing in determining the planetary circulation. Thermal forcing has been overlooked in other studies of persistent long-wave patterns. The study also shows that transient short-waves reorient the planetary scale and add a degree of random or unpredictable behavior. The observational work of Dole (1985) suggests that the onset of persistent anomalies in the Pacific and Atlantic Oceans depends on transient baroclinic events originating at the eastern coast of the continent. The circulation over the oceans which is characterized by a low-frequency maximum downstream of a high-frequency storm track. This circulation undergoes "index-cycle" variability similar to low-order models.

- Charney, J. G. and DeVore, J. G.: Multiple Flow Equilibria in the Atmosphere and Blocking. J. Atmos. Sci., Vol. 36, pp. 1205-1216, 1979.
- Charney, J. G. and Straus, D.: Form-Drag Instability, Multiple Equilibria and Propagating Planetary Waves in the Baroclinic, Orographically Forced, Planetary Wave Systems. J. Atmos. Sci., Vol. 37, pp. 1157-1176, 1980.
- Dole, R. M.: The Life Cycles of Persistent Anomalies and Blocking Over the North Pacific. To appear in Adv. Geophys., 1985.
- Reinhold, B. and Pierrehumbert, R.: Dynamics of the Weather Regimes: Quasistationary Waves and Blocking. Mon. Wea. Rev., Vol. 106, pp. 279-295, 1982.

DAILY SCATTER

$H_2 = .2$ $\theta_2^* = 0$
 $\theta_1^* = .1$ $\theta_5^* = 0$

SAME AS RP
 "DEMONSTRATION CASE".



ORIGINAL PAGE IS
 OF POOR QUALITY

Fig. 1. Amplitudes of the 2 components (sin, cos) of the long wave during a 1000-day model integration. Each point represents the position of the wave in phase space on each day of the experiment. The angle between a ray connecting a daily point with the origin indicates how much the long-wave ridge leads the positive maximum in the forcing (see inset).

Here, the primary weather regimes with unstable zonal flow and topography are a ridge lagging the topographic ridge by 0° to 30° and a ridge leading the topography by 135° (or a trough lagging by 45°).

DAILY SCATTER

$$\begin{aligned} H_2 &= 0 & \theta_1^* &= .05 \\ \theta_2^* &= 0.2 & \theta_5^* &= 0 \end{aligned}$$

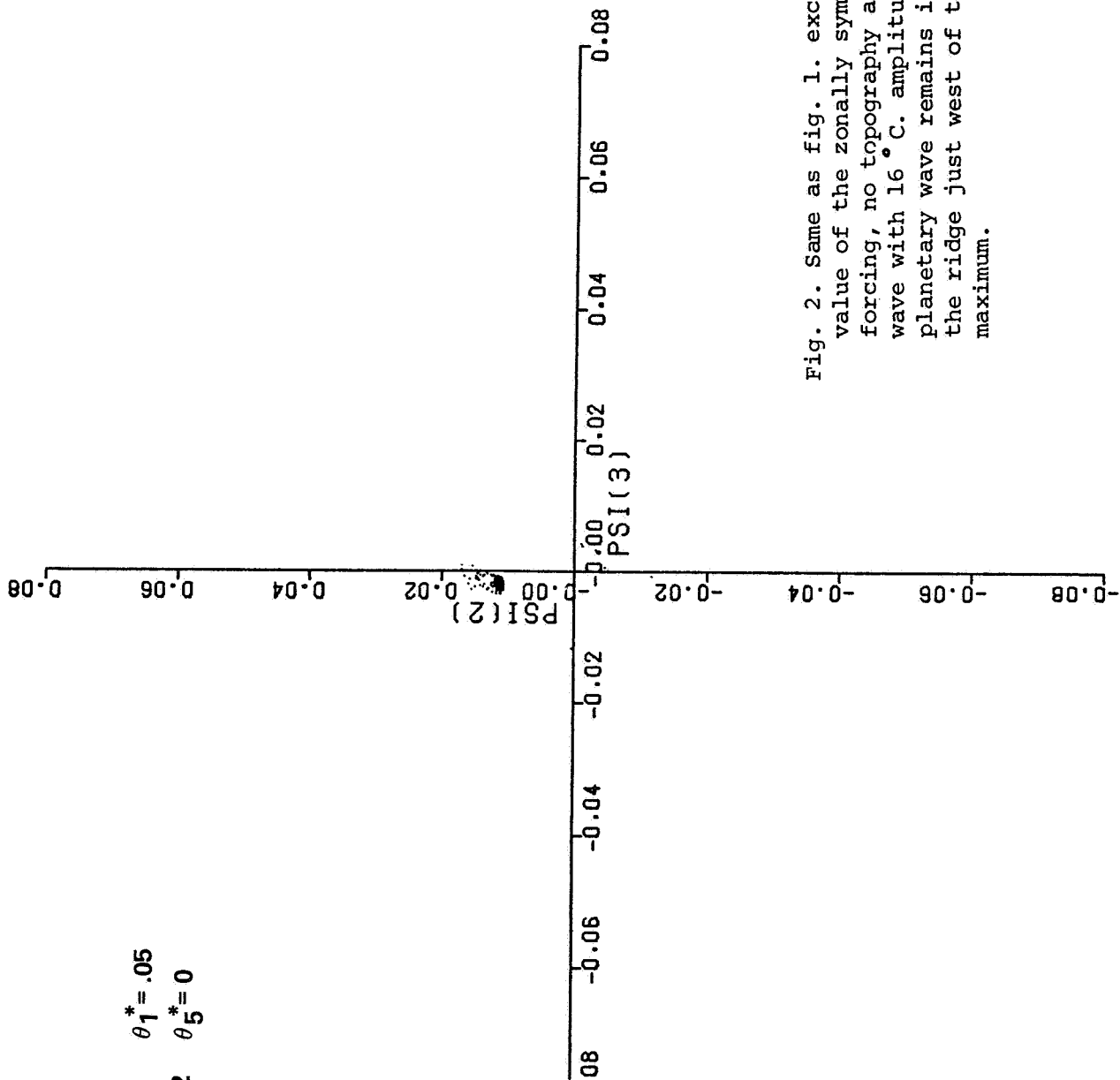


Fig. 2. Same as fig. 1. except for a stable value of the zonally symmetric thermal forcing, no topography and a thermal forcing wave with 16°C amplitude. Note that the planetary wave remains in a steady state with the ridge just west of the thermal forcing maximum.

DAILY SCATTER

$$\begin{aligned} H_2 &= 0 & \theta_2^* &= .02 \\ \theta_1^* &= .1 & \theta_5^* &= 0 \end{aligned}$$

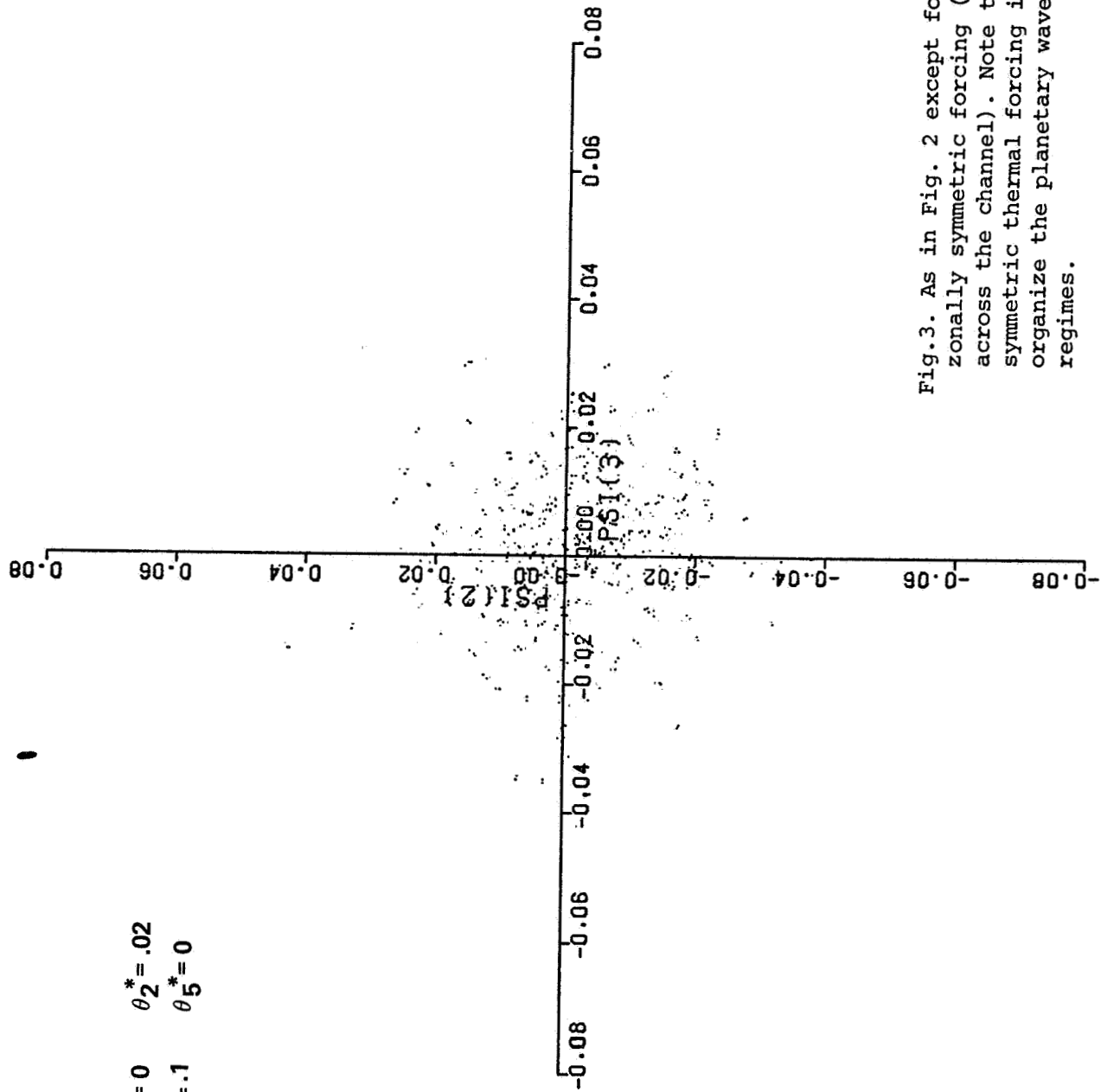


Fig.3. As in Fig. 2 except for an unstable zonally symmetric forcing (60° C. difference across the channel). Note that the non-symmetric thermal forcing is unable to organize the planetary wave into distinct regimes.

DAILY SCATTER

$H_2 = .2$ $\theta_2^* = .02$
 $\theta_1^* = .1$ $\theta_5^* = 0$
 (NEW IC'S)

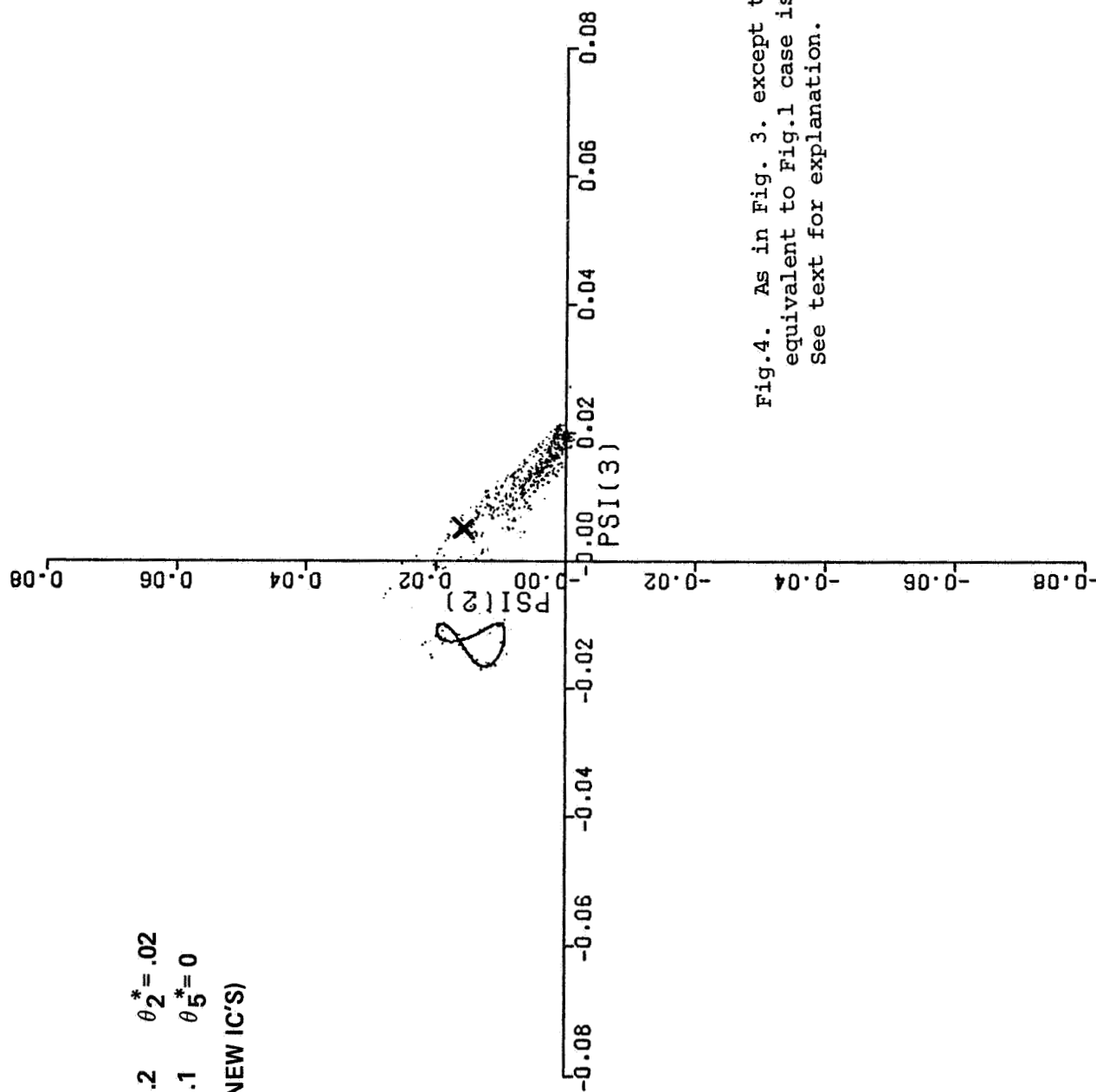


Fig.4. As in Fig. 3. except that topography equivalent to Fig.1 case is included. See text for explanation.

CYCLOGENESIS

Rainer Bleck
University of Miami

Numerical simulations starting from purely zonal initial conditions can be used to show that the baroclinic instability process depicted by classical linear theory leads to precisely the type of mature vortices observed in the extratropical atmosphere. This is not to say, however, that observed cyclones and anticyclones represent the saturation stage of waves grown in an initially undisturbed zonal flow. Rather, baroclinic growth in the atmosphere typically takes place in highly disturbed flow and very often appears to be triggered by a distinct "signal" in the upper-level flow. The interpretation of this signal has changed over the years. In the 1930's (that is, long before the discovery of baroclinic instability) meteorologists knew that the "delta" of a frontal zone is a preferred place for cyclogenesis. The delta is referred to today as the exit region of a jet streak and the jet streak itself is now known to be caused by a local anomaly or "implant" of potential vorticity. Implants of this type, most of which are leftovers of previous cyclogenesis events, are so abundant and so efficient in inducing baroclinic growth that the atmosphere hardly ever is given the opportunity to grow unstable baroclinic waves in textbook fashion from infinitesimal disturbances.

In order to extend the conventional baroclinic instability concept to the situation just described, one has to picture the growth process as resulting from the superposition of two neutrally stable baroclinic waves, an upper and a lower one, each wave propagating along a near-discontinuity in the potential vorticity (PV) field. The PV discontinuity for the lower wave is given by the non-uniformity of the thermal field at the ground, while the discontinuity for the upper wave is given by the contrast, in the 400 to 200 mb range, between the high-PV polar stratosphere and the low-PV subtropical troposphere. Note that the horizontal PV gradients mentioned are approximately opposed to each other, causing the two waves to travel in the opposite direction. As Hoskins et al. (1985) show convincingly, a phase lock between the upper and lower wave may occur, coupled with a tendency toward mutual amplification.

The conceptual model just outlined is particularly attractive to synoptic meteorologists because it does not require the two waves to be of initially small amplitude and thus does not fly in the face of observational evidence. One should also note that this model, by allowing a finite perturbation velocity and a considerable range of relative phase speeds at the time when the upper and lower wave reach the proper phase lag for amplification, may lead to growth rates larger than those predicted by linear theory.

One particular type of cyclogenesis that has received attention lately is the cyclone formation in the lee of mountain ranges like the Alps. Cyclones in that geographical location often start out as mesoscale vortices in a rather homogeneous, warm air mass. Only later do they acquire the size and thermal asymmetry typical of extratropical cyclones. Mattocks and Bleck (1985) have recently speculated that the initial mesoscale growth is not a result of baroclinic instability, but constitutes a geostrophic adjustment process necessitated by the low-level blocking of cold air carried along by a propagating upper-tropospheric jet streak. The authors have demonstrated that the growth rate of the mesoscale lee vortex depends indeed strongly on the intensity of the upper-level potential vorticity implant associated with the jet streak. In order to rule out either baroclinic instability or geostrophic

adjustment as the cause of the pressure fall they are now in the process of diagnosing the sense of the induced ageostrophic circulation. A thermally direct circulation, i.e., ascending warm air and descending cold air, would indicate that the mesoscale vortex is the result of baroclinic instability, whereas a thermally indirect circulation would indicate that the vortex is initiated by uplifting and low-level convergence underneath and to the left of the jet streak as the excess kinetic energy of the jet streak is converted to available potential energy.

References

- Hoskins, B. J., McIntyre, M. E., and Robertson, A. W.: On the Use and Significance of Isentropic Potential Vorticity Maps. Unpublished manuscript, 1985.
- Mattocks, C. A., and Bleck, R.: Geostrophic Adjustment Processes During the Initial Stage of Alpine Lee Cyclogenesis. Submitted to Mon. Wea. Rev., 1985.

EFFECTS OF OROGRAPHY ON PLANETARY SCALE FLOW

Ronald B. Smith
Yale University

The earth's orography is composed of a wide variety of scales, each contributing to the spectrum of atmospheric motions. A well studied subject (originating with Charney and Eliassen) is the direct forcing of planetary scale waves by the planetary scale orography: primarily the Tibetan plateau and the Rockies. However, because of the non-linear terms in the equations of dynamic meteorology, even the smallest scales of mountain induced flow can contribute to the planetary scale if the amplitude of the small scale disturbance is sufficiently large. Two possible mechanisms for this are illustrated in Figure 1. First, preferentially located lee cyclones can force planetary waves by their meridional transport of heat and momentum (Hansen and Chen). Recent theories are helping to explain the phenomena of lee cyclogenesis (e.g., Smith, 1984, J.A.S.). An example is shown in Figure 2. Second, mesoscale mountain wave and severe downslope wind phenomena produce such a large local drag, that planetary scale waves can be produced. The mechanism of upscale transfer is easy to understand in this case as the standing planetary scale wave has a wavelength which depends on the mean structure of the atmosphere, and not on the width of the mountain (just as in small scale lee wave theory). An example of a severe wind flow with very large drag is shown in Figure 3 (Smith, 1985, J.A.S.).

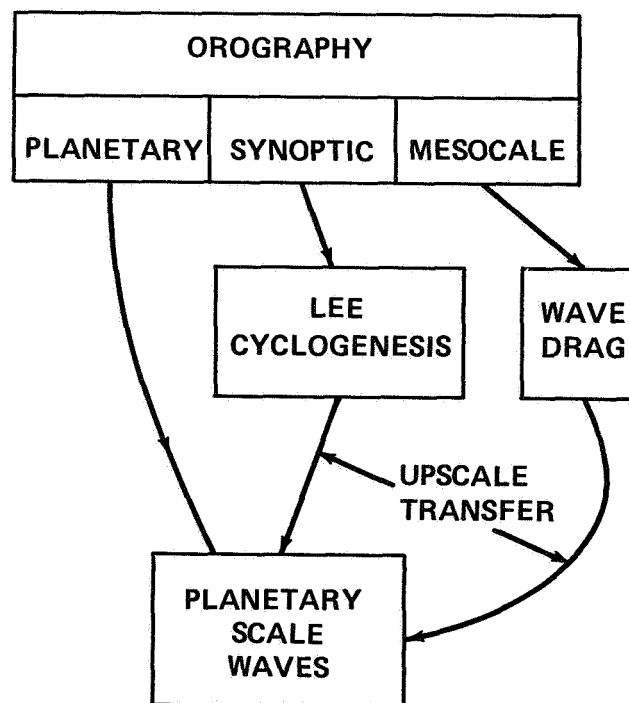


Figure 1.

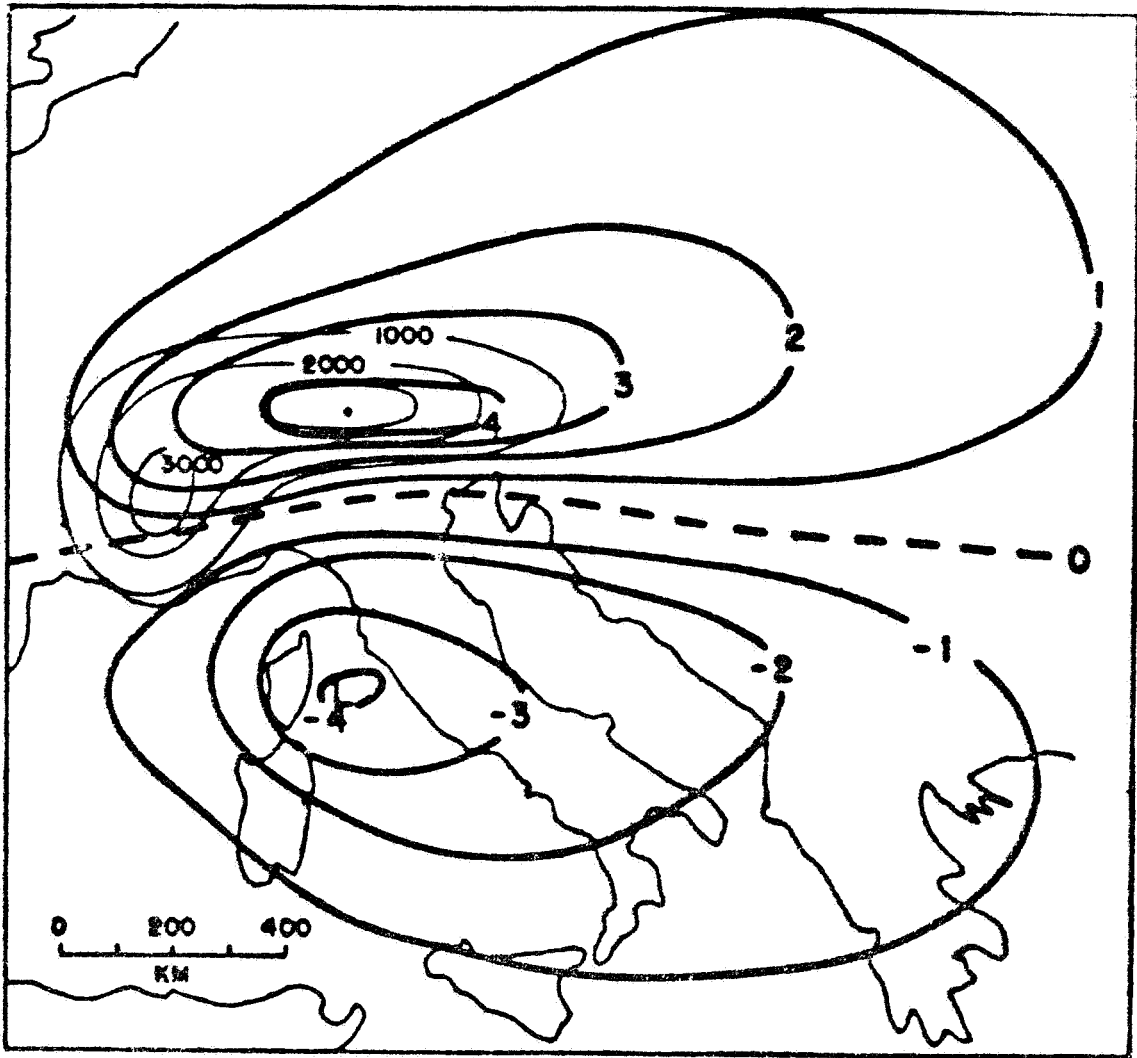


Figure 2

ORIGINAL PAGE IS
OF POOR QUALITY

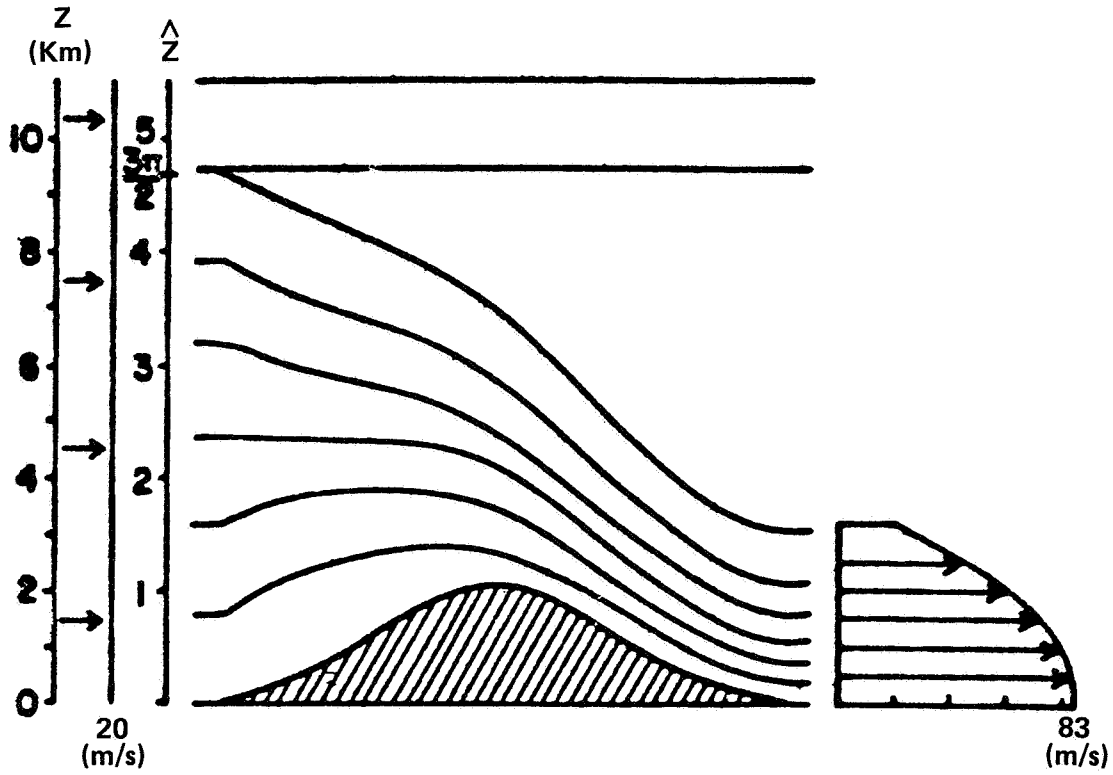


Figure 3.

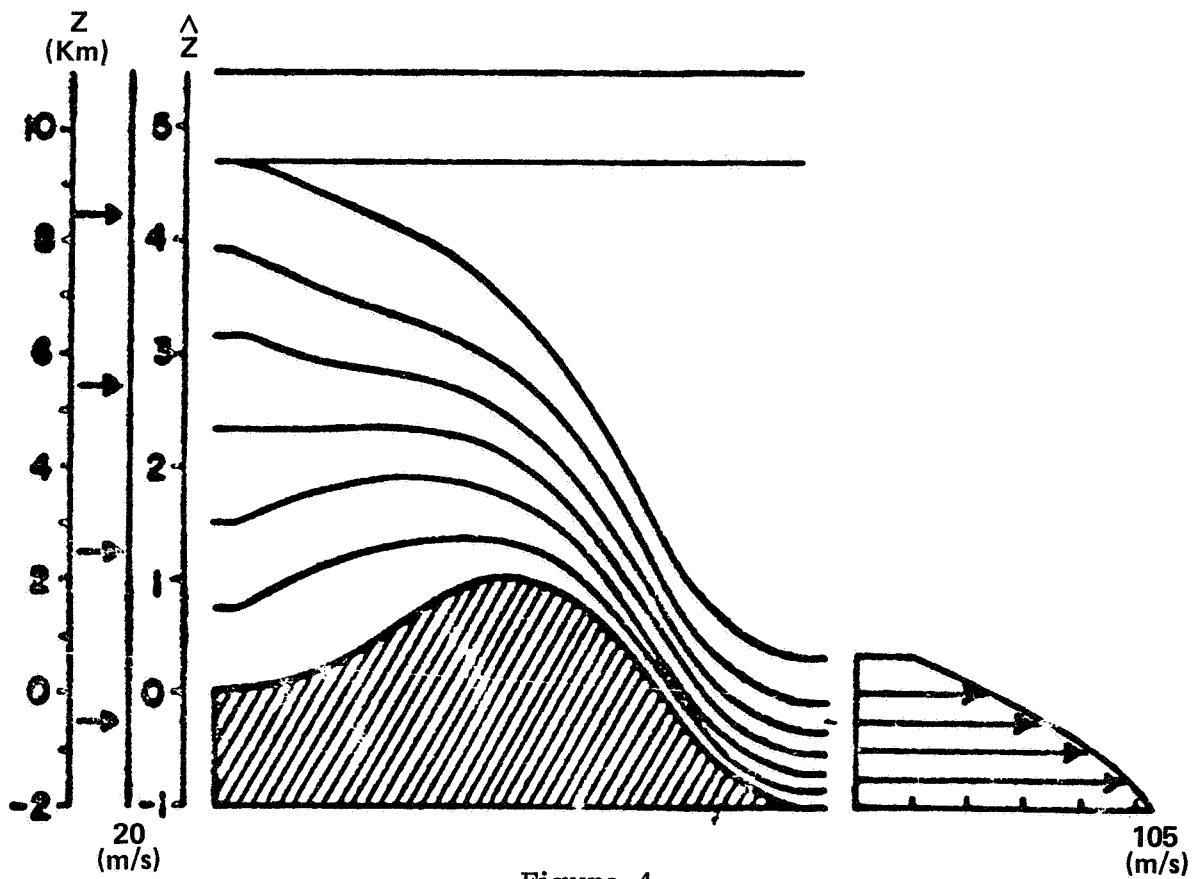


Figure 4

SMALL SCALE FRONTAL STRUCTURE: DYNAMICS OR DETAILS?

David B. Parsons
National Center for Atmospheric Research*
Boulder, CO 80307

1. INTRODUCTION

Today's talk will touch on four topics concerning frontal circulations. The first topic will be a discussion of the results of retrieving pressure and buoyancy perturbations from Doppler radar data taken in an intense surface cold front (Parsons and Gal-Chen, 1985). The second area of discussion will be the presentation of some recent results on instabilities that occur along well defined frontal boundaries (Parsons, 1985). Finally a few words will be presented on the initiation of convection by frontal circulations and the present crisis in our understanding of occluded frontal systems.

2. THE DYNAMICS OF AN INTENSE SURFACE COLD FRONT

A gap exists in our understanding of frontal circulations, since there are very few studies which have adequately explained the nature of frontal circulations on small scales (O kms). Most previous studies of frontal motions fall into two broad categories: analyses that resolve only scales of motion greater than ~ 100 km (includes observational studies using rawinsondes in addition to most numerical and theoretical endeavors) and analyses that resolve the wind field at resolution as small as 1 km but do not include any thermodynamic data on the same scale (specifically Doppler radar studies). In this portion of the talk we will discuss a recent attempt at retrieving pressure and buoyancy data from a wind field derived from data taken using an array of three Doppler radars.

In order to derive pressure and buoyancy data, the technique suggested by Gal-Chen (1978) was employed. Further details can be found in Hane and Scott, 1978; Hane et al., 1981; Roux and Testud, 1983; Gal-Chen and Kropfli, 1985. After application of the anelastic assumption (Batchelor, 1953; Ogura and Phillips, 1962), the momentum equations can be written as:

$$\frac{du}{dt} + f_1 + m_1 \equiv F = -\partial \left(\frac{p'}{\rho_0} \right) / \partial x \quad (1)$$

$$\frac{dv}{dt} + f_2 + m_2 \equiv G = -\partial \left(\frac{p'}{\rho_0} \right) / \partial y \quad (2)$$

$$\frac{dw}{dt} - g\beta' + f_3 + m_3 \equiv H = -\partial \left(\frac{p'}{\rho_0} \right) / \partial z \quad (3)$$

where p' and β' are the deviations in pressure and buoyancy, respectively, from a hydrostatic and adiabatic basic state (always defined by subscript 0). The buoyancy includes the temperature deviation term and the effects of vapor and condensate.

*The National Center for Atmospheric Research is sponsored by the National Science Foundation.

The terms on the left-hand side of equations (1) and (2) can be estimated from the air motions derived from Doppler radar data, if the mixing terms representing the subgrid scale motions can be parameterized. The second moment of the Doppler spectra (Fritsch and Clifford, 1974; Gal-Chen, 1978) can be used to estimate the subgrid terms.

Using these assumptions the horizontal gradients of pressure can be obtained from the Doppler radar measurements. If the data were exact, then either horizontal derivative of pressure and an appropriate boundary condition could be used to derive the actual pressure field. However, the derived winds contain errors from a number of different sources so that the system must be solved in a least squares sense. A Neumann boundary condition was used which allows only for the derivation of a pressure perturbation from its horizontal mean. Once the pressure perturbations are derived, the vertical gradients of pressure deviations are calculated and the buoyancy perturbations are obtained using equation (3).

An alternative investigation into the pressure field involves the derivation of a three-dimensional equation for the pressure (Rotunno and Klemp, 1982). This technique was used for qualitative insight into the physical processes associated with the derived pressure fields. First the pressure (p) is rewritten as $\pi = c_p \theta_0 (p/p_0)^{R/c_p}$, where θ is the potential temperature, c_p is the specific heat constant at constant pressure, and R the universal gas constant. Next equations (1) through (3) are rewritten in shallow form. A three-dimensional elliptical equation can be obtained by taking the divergence of the momentum equations (modified equations (1) through (3)) and using the continuity equation. The resulting equation is given by

$$\begin{aligned} & \left(\frac{\partial u}{\partial x} \right)^2 + \left(\frac{\partial v}{\partial y} \right)^2 + \left(\frac{\partial w}{\partial z} \right)^2 + 2 \left(\frac{\partial u}{\partial y} \right) \left(\frac{\partial v}{\partial x} \right) \\ & + 2 \left(\frac{\partial u}{\partial z} \right) \left(\frac{\partial w}{\partial x} \right) + 2 \left(\frac{\partial v}{\partial z} \right) \left(\frac{\partial w}{\partial y} \right) - \frac{\partial \beta'}{\partial z} \\ & + \nabla(f_1 + f_2 + f_3 + m_1 + m_2 + m_3) = -\nabla^2 \pi \end{aligned} \quad (4)$$

As described previously, all the terms on the left side of equation (4) can be calculated from the Doppler radar measurements except the buoyancy term ($\partial \beta' / \partial z$). This term can be separately calculated as in Brandes (1984) or estimated from the previous calculation and an appropriate boundary condition.

The cold front discussed in this section has been detailed in Carbone (1982, 1983). The system passed through central California on 5 February 1978 producing heavy rain and a weak tornado. Data were taken using three Doppler radars and serial rawinsonde ascents as part of the Sierra Project. Excellent spatial resolution was obtained as the wind fields were interpolated to a 300 m three-dimensional grid at four different times. An example of the average flow characteristics associated with the front is shown in Figure 1a. The boundary layer ahead of the front is dominated by strong relative flow towards the front. This flow decelerates into an intense (locally $> 20 \text{ ms}^{-1}$) updraft at the leading edge of the cold front. The region of high radar reflectivity and the updraft are quite shallow. The cold air mass

appears in a shape similar to a density current with a steep leading edge, a frontal head, and a relatively flat slope behind this head. The region within the head contains a closed circulation with ascent at the leading edge of the cold front and descent behind the head. A maximum in the horizontal flow towards the also occurs in the lower layer within the head.

The pressure field averaged along the front revealed a number of interesting aspects of the frontal circulation (Fig. 1b). At the leading edge of the cold front a region of high pressure is present in the low levels. In the region toward the top of the cold front a low pressure area dominated the pressure field. The typical magnitude of these pressure changes are a ~ 1 mb in a few kilometers indicating a balance between the accelerations of the wind and the horizontal pressure gradients. The high along the leading edge of the front produces a geostrophic flow with northerlies ahead of the front and southerlies in the post-frontal air mass. However, the observed flow contained an intense southerly low-level jet in the warm-sector and weak northerlies behind the front. Hence, the along front wind is highly ageostrophic and the assumption of along front geostrophy, which is often used in conjunction with the semi-geostrophic equations, is clearly violated. Also, since the high pressure at the leading edge of the front extends into the warm-sector, the pressure rise would not be solely due to the hydrostatic effects of the advancing cold air mass. Another implication of the pressure field is the strong upward directed pressure force within the frontal updraft, suggesting that pressure perturbations must be accounted for in order to explain the intense updrafts.

While these implications are interesting, the validity of the pressure fields must be proven. Four separate tests for the quality of the data were taken. Since the results were derived in a least squares sense, a comparison of the derived pressure gradients with the input values provides the first test. While there is not sufficient space for details, this comparison suggests that the data is as consistent as the best published results. Of course the observations provide the ultimate truth for the retrieval process. The pressure field measured at the surface indicates similar trends and magnitudes as the derived results for the lowest plane of derived data. A third test of the retrieval process is the derivation of buoyancy perturbations, since the buoyancy values suggests 3°K in cooling across the front. This value is quite similar to the difference observed in the sounding data again indicating a realistic pressure field. Interestingly, the cooling starts within the updraft ahead of the front so that the intense updraft is not buoyant in the conventional sense. This result is expected from the sounding data but is somewhat controversial due to the large magnitude of the updraft.

The fourth test of data quality was a numerical simulation. A 2-D version of the MRS cloud model (Klemp and Wilhelmson, 1978) was used in the simulations with a 250 m grid. Various stabilities were chosen for the warm-sector air mass and the cold air mass was initialized with temperature deficits below a height similar to that of the depth of the observed cold air mass. The flow and pressure field rapidly take on a structure quite similar to the observations with a high in the low levels and a low aloft. Interestingly, an examination of equation (4) for the data and simulations indicate an identical interpretation for the two pressure fields. The high at leading edge of the front is consistent with the first three terms in equation (4) and can physically be thought of as forced convergence at the leading edge of the front. The updrafts were non-buoyant compared to the warm-sector air mass consistent with the terms associated with a horizontal gradient in the vertical motion and a vertical shear in the horizontal winds [in a system with the x axis perpendicular to the front the fifth term in equation (4)]. This term can be thought of as rotation about an

axis parallel to the horizontal alignment of the front. In both the observations and simulations coriolis was generally not important and the front can be thought of as behaving in a manner analogous to a density current (e.g., Simpson, 1969). The results of other studies such as Shapiro, et al. (1985), suggest that this type of front that has collapsed to a sharp discontinuity represents a distinct and common class of fronts in the atmosphere for moist and dry circulations despite the recent results that suggest such sharp fronts may be difficult to produce in the atmosphere (Orlanski and Ross, 1984).

3. NON-TWO DIMENSIONAL FRONTS

Recently, investigators have examined the three-dimensional aspects of frontal convection (Hobbs and Biswas, 1979; James and Browning, 1979; Emanuel, 1980; Carbone, 1982; Hobbs and Persson, 1982; Parsons and Hobbs, 1983a,b). A substructure was found which most often took the form of cores of intense precipitation typically appearing at rather regular intervals with spacings along the front of approximately 15 km. A number of investigators have proposed that these precipitation areas are the manifestation of a wave that derives its energy source from the intense shear in the horizontal wind across the surface cold front. Hence we will call these disturbances frontal shear waves (FSW's).

However, there is some evidence in the literature that a second disturbance may be present in the data. This disturbance has spacings along the front of ~ 75 km. Due to the scale of this second disturbance and due to other reasons that will become clear later we will call this 75 km disturbance a frontal mesoscale wave (FMW). The first suggestion of FMW's patterning the frontal precipitation can be found in James and Browning (1980). In this study the authors found that the precipitation "elements vary in length from a few kilometers to more than 100 km." The authors also found a tendency for the larger scale features to be much longer lived than those elements with smaller scales but did not suggest that two scales of disturbance were present. The only evidence for two different disturbances with two scales of motion present was the mention that the larger disturbances tend to be often subdivided. The case for a second larger scale disturbance was made clearer by Carbone (1982) (the case used in Section 2), who studied a cold frontal squall line using multiple Doppler radar data. Carbone found a smaller wave with along front spacings on the order of 15 km and a larger one with a wavelength of nearly 75 km (see Figs. 2 and 3 in Carbone, 1982). Unfortunately the area of multiple Doppler coverage was far smaller than the 75 km wavelength of the FMW's and Carbone's study concentrated exclusively on the scale of the FSW's.

The picture at the present time is unclear. It is not certain whether two scales of disturbances are often present within well defined frontal systems or whether Carbone's case was an isolated one forced by topography or the intense convection. It is also not clear whether these disturbances interact with each other or if they significantly pattern the convection. Also the forcing mechanisms for these disturbances (especially the longer wave length disturbance) are unclear. In this section the results of an examination of the substructure of six well defined cold fronts will be summarized.

The results have suggested that two different scales of disturbance are common along the surface cold fronts. The characteristics of the FSW's were not surprising: the along front spacing was 13 km and the features moved along the surface front with a wind velocity representative of the frontal zone. A detailed three-dimensional examination of the pressure data discussed in the past section reveals a pronounced pressure signal associated with 13 km disturbance. The along front variations

associated with the disturbance were in excess of 1 mb and explain the significant along front variation observed in the pressure field associated with cold fronts. These pressure differences were a maximum in the lower levels and decreased slowly with height above the top of the frontal zone. Other more detailed analysis of the disturbance structure for this case is underway.

The wavelength of the FMW's was found to be approximately 80 km. This disturbance also moved along the front with the wind speed within the frontal zone. An interesting characteristic of these disturbances is their tendency to be more clearly evident in cases with an inversion in the warm-sector. The Rossby number for this disturbance was approximately 1, making this disturbance a truly mesoscale phenomenon. Another aspect of the FMW's is their ability to pattern both the convection and the preferred location of the FSW's presumably from altering the background convergence and vorticity fields (Fig. 2). The mechanism for this disturbance is unclear and numerical work is underway in this area.

4. FRONTS AND CONVECTION

The preceding discussion has a great deal of impact on our understanding of the interaction between fronts and convection. Clearly the synoptic scale secondary circulations measured in terms of $1-10 \text{ cm s}^{-1}$ appear to be rather ineffective in releasing convective instability when compared to the vertical motions present at the nose of the front ($1-10 \text{ m s}^{-1}$). However, a direct comparison of the magnitude of the vertical motion may not be appropriate since the intense vertical motions are quite shallow and often below the level of free convection. The vertical motion pattern associated with the FSW's and FMW's may also be important since these disturbances pattern the vertical motion fields in less unstable cases. Observations were taken recently with instrumented aircraft and Doppler lidar in west Texas (led by M. Shapiro, NOAA/ERL) in an attempt to clarify current understanding of the role of frontal forcing in initiation of convection.

5. A CRISIS IN OCCLUSIONS

In concluding this talk a few words concerning occluded frontal systems are in order. The numerical work of Hoskins and West (1979) has shown that our old synoptic ideas concerning the development of occlusions are dated since the cold air mass was not observed to overtake the warm front to form an occlusion. Instead the air within the warm-sector decreased with time due to the upward movement of warm air which is necessary for the growth of the baroclinic disturbance. Since Krietzberg and Brown (1970) observational analysis tend to show that occlusions are often dominated by mesoscale circulations that aid the upward transport of the warm air with time. The role of this mesoscale transport in the maintenance of the baroclinic disturbance and a host of other questions remain to be answered as our understanding of occluded systems waits to be redefined.

6. REFERENCES

- Batchelor, G. K.: The Condition for Dynamical Similarity of Motions of a Frictionless Perfect-Gas Atmosphere. *Quart. J. R. Meteor. Soc.*, Vol. 79, 1953, pp. 224-235.
- Brandes, E. A.: Vertical Vorticity Generation and Mesocyclone Sustenance in Tornadoic Thunderstorms: The Observational Evidence. *Mon. Wea. Rev.*, Vol. 112, 1984, pp. 2253-2269.
- Carbone, R.: A Severe Winter Squall Line. Part 1: Stormwide Hydrodynamic Structure. *J. Atmos. Sci.*, Vol. 39, 1982, pp. 258-279.
- Carbone, R.: A Severe Winter Squall Line. Part 2: Tornado Parent Vortex Circulation. *J. Atmos. Sci.*, Vol. 40, 1983, pp. 2639-2654.
- Emanuel, K. A.: Forced and Free Mesoscale Motions in the Atmosphere. Collection of Lecture Notes on Dynamics of Mesometeorological Disturbances. *Proc. CIMMS Symposium*, University of Oklahoma Press, 1980, pp. 191-259.
- Fritsch, A. S., and Clifford, S. F.: A Study of Convection Capped by Stable Layer Using Doppler Radar and Acoustic Echo Sounder. *J. Atmos. Sci.*, Vol. 31, 1974, pp. 1622-1628.
- Gal-Chen, T.: A Method for the Initialization of the Anelastic Equations: Implications for Matching Models with Observations. *Mon. Wea. Rev.*, Vol. 106, 1978, pp. 587-696.
- Gal-Chen, T., and Kropfli, R. A.: Buoyancy and Pressure Perturbations Derived from Dual-Doppler Radar Observations of the Planetary Boundary Layer: Application for Matching Models with Observations. *J. Atmos. Sci.*, Vol. 41, 1985, pp. 3007-3020.
- Hane, E. E., and Scott, B. C.: Temperature and Pressure Perturbations Within Convective Clouds Derived from Detailed Air Motion Information: Preliminary Testing. *Mon. Wea. Rev.*, Vol. 109, 1978, pp. 564-576.
- Hane, E. E., Wilhelmson, R. B., and Gal-Chen, T.: Retrieval of Thermodynamic Variables Within Deep Convective Clouds: Experiments in Three Dimensions. *Mon. Wea. Rev.*, Vol. 109, 1981, pp. 564-576.
- Hobbs, P. V., and Biswas, K. R.: The Cellular Structure of Narrow Cold Frontal Rainbands. *Quart. J. Roy. Meteor. Soc.*, Vol. 105, 1979, pp. 723-727.
- Hobbs, P. R., and Persson, P. O. G.: The Mesoscale and Microscale Structure of Clouds and Precipitation in Midlatitude Cyclones. V. The Substructure of Narrow Cold Frontal Rainbands. *J. Atmos. Sci.*, Vol. 39, 1982, pp. 280-295.
- Hoskins, B. J., and West, N. V.: Baroclinic Waves and Frontogenesis. Part 2: Uniform Potential Vorticity Jet Flows-Cold and Warm Fronts. *J. Atmos. Sci.*, Vol. 36, 1979, pp. 1663-1680.
- James, P. K., and Browning, K. A.: Mesoscale Structure of Line Convection at Surface Cold Fronts. *Quart. J. Roy. Meteor. Soc.*, Vol. 105, 1979, pp. 371-382.

- Klemp, J. B., and Wilhelmson, R. B.: The Simulation of Three-Dimensional Convective Storm Dynamics. *J. Atmos. Sci.*, Vol. 35, 1979, pp. 1070-1096.
- Krietzberg, C. W., and Brown, H. A.: Mesoscale Weather Systems Within an Occlusion. *J. Appl. Meteor.*, Vol. 9, 1970, p. 417-432.
- Ogura, Y., and Phillips, N. A.: Scale Analysis of Deep and Shallow Convection in the Atmosphere. *J. Atmos. Sci.*, Vol. 19, 1962, pp. 173-179.
- Orlanski, I., and Ross, B. B.: The Evolution of an Observed Cold Front. Part II: Mesoscale Dynamics. *J. Atmos. Sci.*, 1984, pp. 1669-1703.
- Parsons, D. B.: Evidence for a Mesoscale Disturbance Along Surface Cold Frontal Zones. *Programs/Abstracts 2nd Conf. on Mesoscale Processes*, Amer. Meteor. Soc., Boston, MA, Vol. 23, 1985.
- Parsons, D. B., and Hobbs, P. V.: The Mesoscale and Microscale Structure of Clouds and Precipitation in Midlatitude Cyclones. VII: Formation, Development, Interaction, and Dissipation of Rainbands. *J. Atmos. Sci.*, Vol. 40, 1983, pp. 559-579.
- Parsons, D. B., and Hobbs, P. V.: The Mesoscale and Microscale Structure of Clouds and Precipitation in Midlatitude Cyclones. XI: Comparison Between Observational and Theoretical Aspects of Rainbands. *J. Atmos. Sci.*, Vol. 40, 1983, pp. 2377-2397.
- Parsons, D. B., and Gal-Chen, T.: The Dynamics of an Intense Surface Front. *Programs/Abstracts 2nd Conf. on Mesoscale Processes*, Amer. Meteor. Soc., Boston, MA, 1985.
- Rotunno, R., and Klemp, J. B.: The Influence of the Shear-Induced Pressure Gradient on Thunderstorm Motion. *Mon. Wea. Rev.*, Vol. 110, 1982, pp. 136-151.
- Roux, F., and Testud, J.: Pressure and Temperature Fields Retrieved from Dual-Doppler Radar Data. An application to the observation of a West African squall-line. *Preprints 21st Conf. on Radar Meteor.*, Edmonton, Alta., Canada, Amer. Meteor. Soc., Boston, MA, 1983, pp. 20-31.
- Shapiro, M. A., Hampell, T., Rotzell, D., and Mosher, F.: The Frontal Hydraulic Head: A Micro-Alpha Scale (~ 1 km) Triggering Mechanism for Mesoconvective Weather Systems. *Mon. Wea. Rev.*, (in press) 1985.
- Simpson, J. E.: A Comparison Between Laboratory and Atmospheric Density Currents. *Quart. J. Roy. Met. Soc.*, Vol. 95, 1969, pp. 758-765.

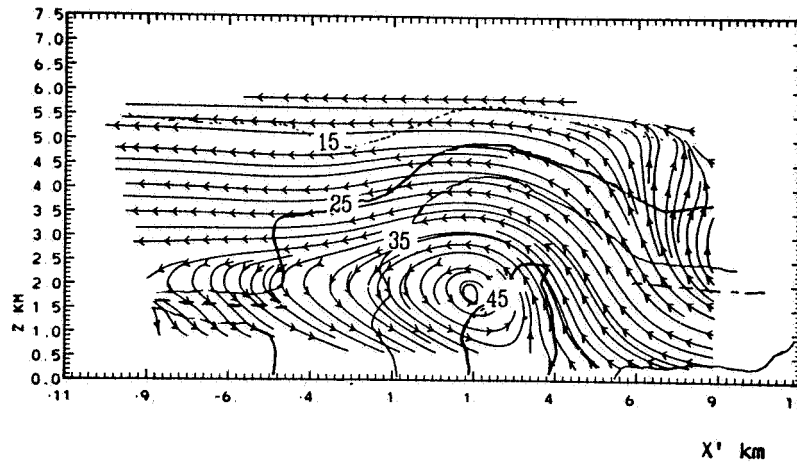


Fig. 1a

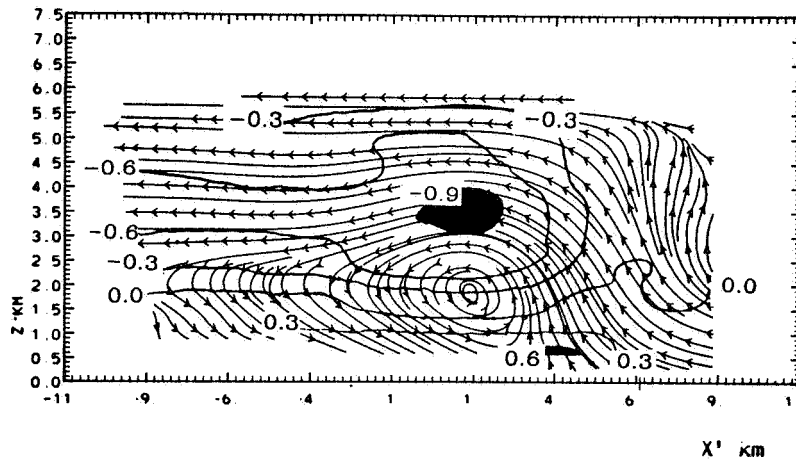


Fig. 1b

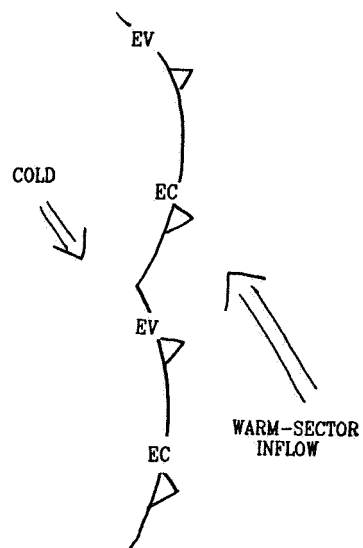


Fig. 2

SIMULATIONS OF GRAVITY WAVES IN FRONTAL ZONES

Robert Gall

Recent observations of frontal systems passing over the PROFS network in Colorado by Shapiro (1984) indicate the horizontal scale of some fronts can be on the order of a few kilometers or less. This result has been further explored in even more recent work, some of which was reported, at this meeting by Parsons. Motivated by Shapiro's results we re-ran an earlier numerical simulation of frontogenesis by Williams (1972) (where a very simple stretching deformation forcing of a front is considered) using as high a resolution in both the vertical and horizontal as was possible. Highest resolution that we considered consisted of a grid with a vertical spacing of 32 meters and a horizontal spacing of 260 meters in the immediate vicinity of the surface front. The purpose was to examine development of the frontal structures as the scale of the front became very small.

Because we were interested in simulating very small scale features we chose to use the non-hydrostatic cloud model described by Clark (1977). This model has a number of attractive features including (1) it can easily be transformed into a form suitable for two-dimensional frontal solutions, and (2) three levels of full interactive nesting is possible. This latter feature allows high resolution in some regions while permitting low resolution in regions where it is warranted. For the frontal calculations considered here, small scale motions only develop in a very restricted region near the lower and upper boundaries. Thus, the high resolution inner model need only cover a very small area even though the front is forced by large scale motions.

The procedure for achieving the high resolution simulations was to first integrate a relatively low resolution model until higher resolution was needed as the front collapsed. Then using the results at that time a higher resolution model was initialized from the low resolution model and the integration continued. Near the time when the front approaches a discontinuity, high resolution inner models are initialized in the vicinity of the surface front, first one inner nested model, then two.

One result of this calculation was that the very fine horizontal structures reported by Shapiro did not develop. The slope of our simulated front is very shallow $1/140$. Since the scale of the front is contracting both vertically and horizontally, this shallow slope means that the vertical resolution stops the frontal collapse before the horizontal scale of the front is affected by the horizontal resolution in our simulation. For the minimum vertical resolution used (35 meters) this meant that the horizontal scale only contracts to about 3 km. It is possible that if surface stress had been included, the front would have taken on a much steeper slope near the surface allowing front to collapse to the horizontal resolution.

In spite of our failure to reach very fine scales, there is a very interesting result concerning the generation of gravity wave motion within the collapsing front. As the front collapses, non-hydrostatic and non-geostrophic accelerations develop in the frontal zone. They are the result of the continual changing of the mass and momentum fields within the front. These accelerations increase as the frontogenesis progresses, presumably approaching infinity if the front could actually go to a discontinuity. Furthermore, since the frontogenesis is a maximum at the boundary, these accelerations are largest there, decreasing upward along the frontal surface.

These accelerations will, of course, result in the generation of gravity wave energy as has already been discussed to some extent by Ley and Peltier (1978). They considered wave motion, so generated, as it would appear far from the front. However, in some ways the wave motion generated by the front in the immediate vicinity of the front is perhaps even more interesting.

In a typical surface front (including the one considered here) the flow above the front is toward the cold side of the surface front and while the flow below the front is cold toward warm. Because the mean flow in these regions is non-zero, stationary waves generated by the accelerations in the frontal zone are possible. For example, above the frontal surface, stationary waves would have phase line tilting toward the warm air with height since they must propagate upward away from their source in the front and they would have a vertical wavelength approximately.

$$L_z = \frac{2\pi N}{U} \quad (1)$$

For typical values of N and U of the flow over our front, L_z will be about 2 km.

Figure 1 shows the development of the stationary waves above the frontal surface as time progresses. They first appear at the position of the nose of the front (at around -430 km in the diagram) and then build upward (with the vertical group velocity) and intensity as well as spread backward along the front. Because the waves are nearly hydrostatic (due to their large horizontal scale ~ 50 km) the stationary waves appear only above their source. Note that some weak traveling waves are apparent ahead of the front as well. The vertical wavelength is about 2 km as suggested by Equation (1). The horizontal wavelengths appear to be determined by the horizontal scale of the frontal zone.

Below the front, because of the presence of the lower surface, standing waves become possible. In other words reflections between the frontal surface where the flow perpendicular to the front is zero and the ground are possible. Again, the vertical wavelength of the waves that are stationary (and therefore will stand under the front) are given by Equation (1). Boundary conditions at the surface and the front then demand that the standing waves will only occur where the height of the frontal surface above the ground is an integer multiple of $L_z/2$. This and the slope of the front will then determine the horizontal scale of the standing wave which for our simulation is about 50 km. In other words the first wave will occur about 50 km behind the nose of the front (see Fig. 2).

With continuous forcing the waves under the front increase in amplitude until non-linear processes become important, causing the waves to break. In effect smaller versions of the frontogenesis process proceed within the standing waves. As these standing waves under the front break, additional sources of gravity wave energy develop and additional stationary waves develop above these regions (Fig. 3). Figures 2 and 3 show the development of the standing waves under the front (note circulation at -350 km) and the breaking waves.

We suggest that waves such as described above may explain at least some of the banding often observed in the clouds along frontal zones, especially those where there is little precipitation. In such zones symmetric instability is unlikely yet gravity wave production will occur and could introduce a banded structure in those clouds that are present. There are two sources for the banding: (1) the stationary waves above the front and (2) waves propagating upward from the breaking waves under the front.

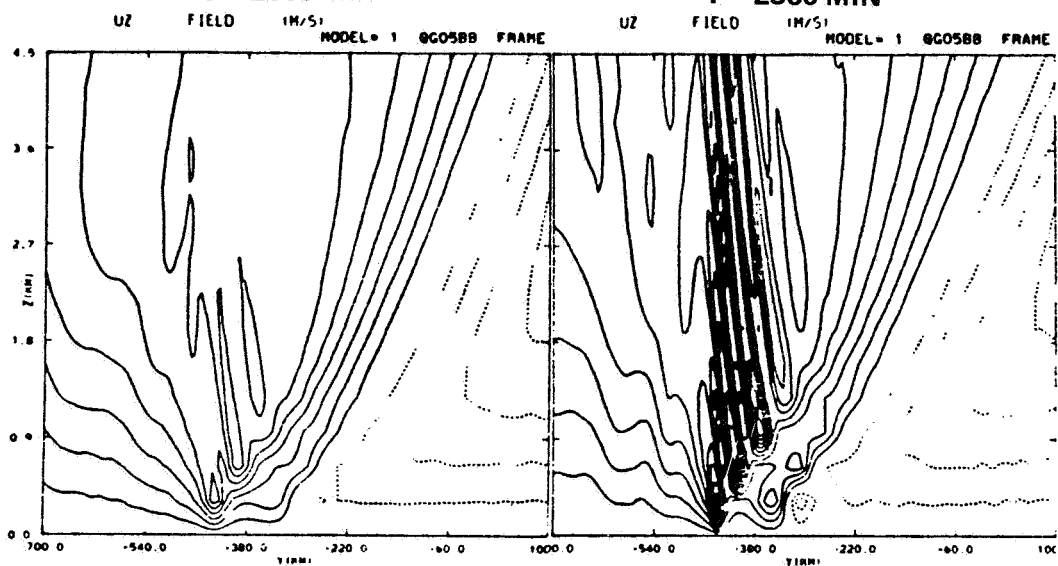
REFERENCES

- Clark, T. L., 1977: A Small-Scale Dynamic Model Using a Terrain Following Coordinate System. *J. Comp. Phys.*, Vol. 26, pp. 186-215.
- Ley, B. E., and Peltier, W. R., 1978: Wave Generation and Frontal Collapse. *J. Atmos. Sci.*, Vol. 35, pp. 3-17.
- Shapiro, M. A., 1984: Meteorological Tower Measurements of a Surface Cold Front. *Mon. Wea. Rev.*, Vol. 112, No. 8.
- Williams, R. T., 1972: Quasi-Geostrophic Verses Non-Geostrophic Frontogenesis. *J. Atmos. Sci.*, Vol. 29, p. 3-10.

ORIGINAL PAGE IS
OF POOR QUALITY

T = 2060 MIN

T = 2360 MIN



T = 2540 MIN

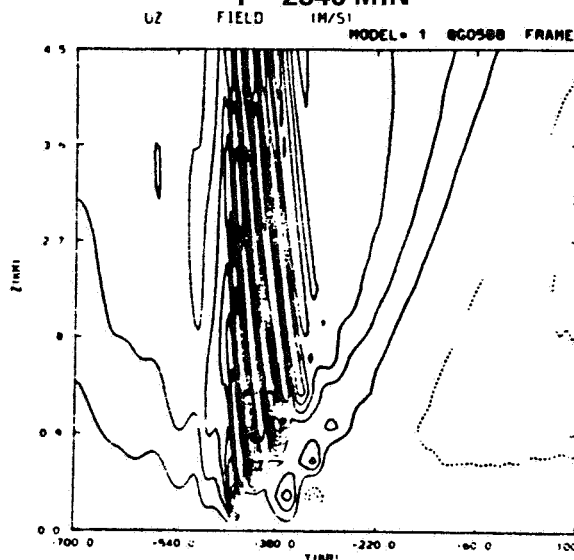


Figure 1. Vertical wind component, U_z (m/sec) at various times from beginning of experiment. Measure on bottom axis is distance from axis of dilation. In this experiment $\Delta y = 5.0$ km, $\Delta z = 320$ m.

REPRODUCED AT GOVERNMENT EXPENSE

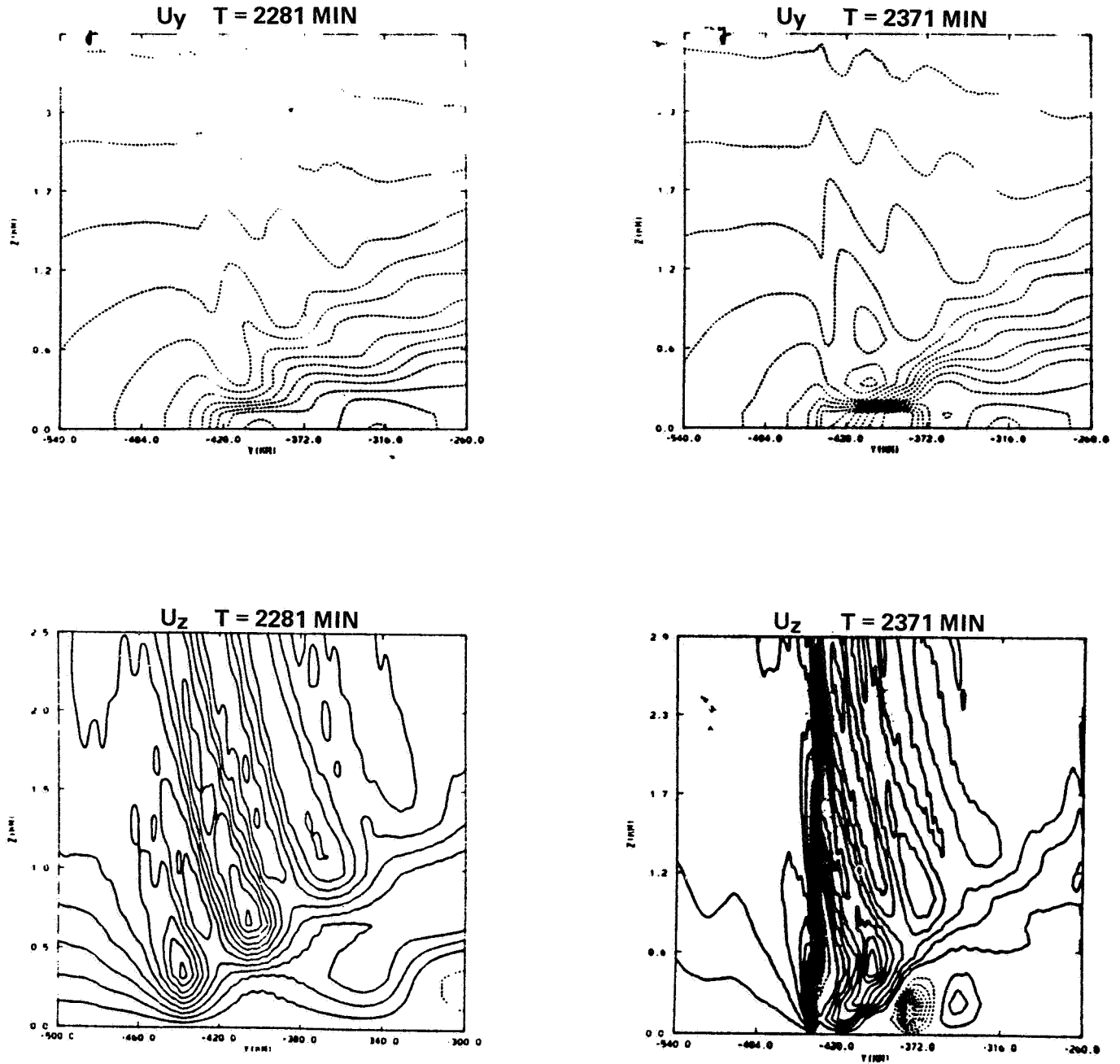


Figure 2. Perturbation wind component perpendicular to the front U_y (m/sec), top and vertical wind component U_z (m/sec), bottom, at various times from beginning of experiment. Measure on bottom axis is distance from axis of dilation. In this experiment $\Delta y = 833$ m, $\Delta z = 110$ m.

ORIGINAL PAGE IS
OF POOR QUALITY

ORIGINAL PAGE IS
OF POOR QUALITY

REPRODUCED AT GOVERNMENT EXPENSE

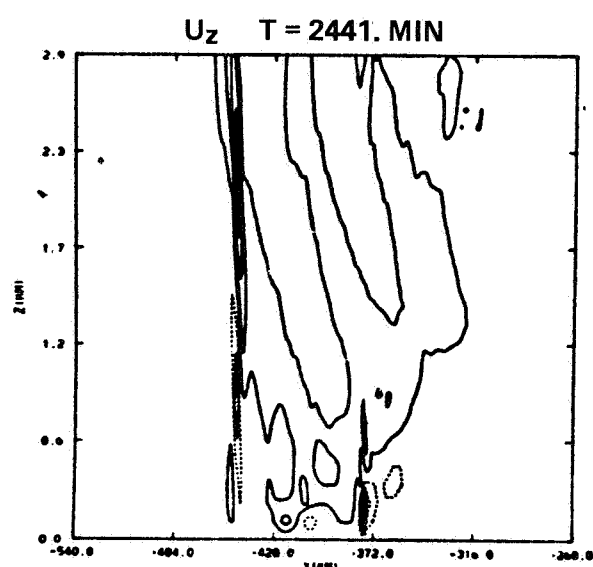
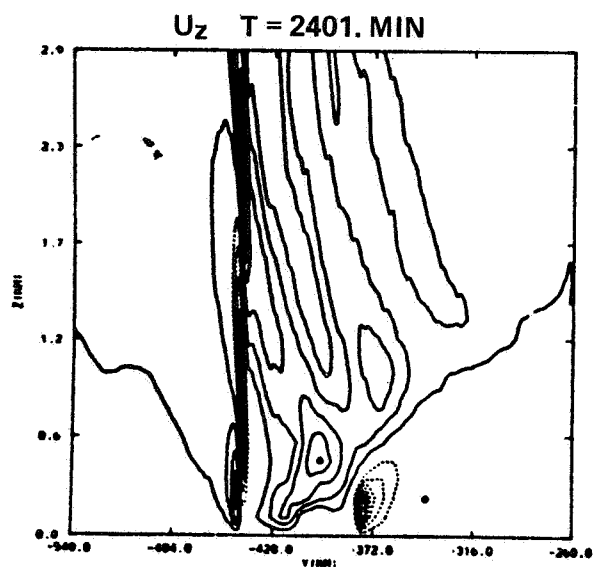
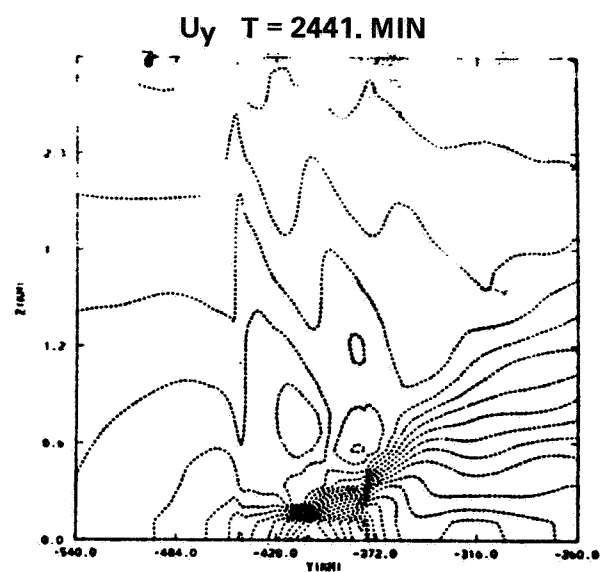
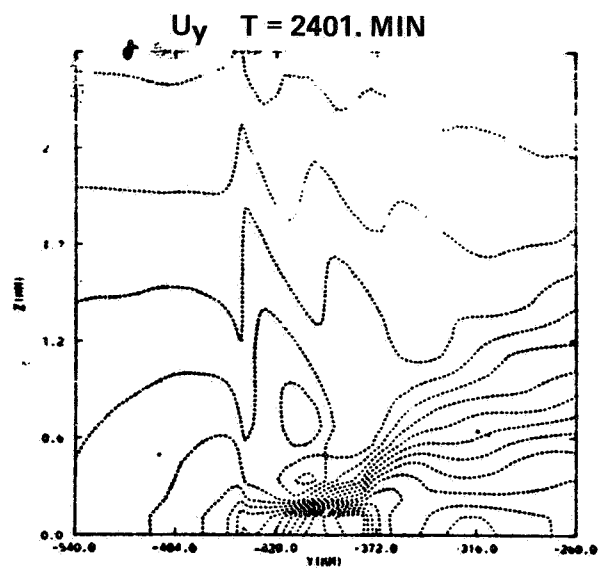


Figure 3. Same as Figure 2.

1. REPORT NO. NASA CP-2410		2. GOVERNMENT ACCESSION NO.		3. RECIPIENT'S CATALOG NO.	
4. TITLE AND SUBTITLE Current Scientific Issues in Large Scale Atmospheric Dynamics				5. REPORT DATE January 1986	
				6. PERFORMING ORGANIZATION CODE	
7. AUTHOR(S) Timothy L. Miller, Compiler				8. PERFORMING ORGANIZATION REPORT #	
9. PERFORMING ORGANIZATION NAME AND ADDRESS George C. Marshall Space Flight Center Marshall Space Flight Center, Alabama 35812				10. WORK UNIT NO. M-506	
				11. CONTRACT OR GRANT NO.	
12. SPONSORING AGENCY NAME AND ADDRESS National Aeronautics and Space Administration Washington, D.C. 20546				13. TYPE OF REPORT & PERIOD COVERED Conference Publication	
				14. SPONSORING AGENCY CODE	
15. SUPPLEMENTARY NOTES Prepared by Systems Dynamics Laboratory, Atmospheric Sciences Division.					
16. ABSTRACT A workshop was held June 20 and 21, 1985, at Marshall Space Flight Center, for the purpose of exploring areas of research in global scale atmospheric dynamics which might be valuable additions to the research program at the Atmospheric Sciences Division, Systems Dynamics Laboratory. There were 12 invited participants from universities and other institutions. The topics were (1) persistent anomalies ("blocking"), (2) cyclogenesis and mountain effects, and (3) frontal dynamics. Abstracts of two talks per topic are included in this publication.					
17. KEY WORDS Atmospheric dynamics Cyclogenesis Atmospheric blocking Frontal dynamics			18. DISTRIBUTION STATEMENT Unclassified - Unlimited Subject Category 47		
19. SECURITY CLASSIF. (of this report) Unclassified		20. SECURITY CLASSIF. (of this page) Unclassified		21. NO. OF PAGES 44	
				22. PRICE A03	